

Conversion of Light to Matter

M. Pentia – WQD 18 April 2024

Outline

1. Introduction
2. Vacuum interactions – Schwinger effect
3. QED interaction processes (theory & exp.)
4. ELI-NP Experiments for SF-QED study
5. Physics of the QED processes at ELI-NP
6. Task Force, plan and resources

1.1 QED History at ELI-NP

Dream 2009

G. V. Dunne (University of Connecticut) in the paper “*New strong-field QED effects at extreme light infrastructure*” in Eur. Phys. J. D 55, 327–340 (2009) remarked “**the ELI project open up an entirely new non-perturbative regime of QED, and of quantum field theories in general.** There are many experimental and theoretical challenges ahead. Theoretically, the biggest challenge in the non-perturbative arena is to develop efficient techniques, both analytical and numerical, for computing the effective action and related quantities, in external fields that realistically represent the experimental laser configurations. A lot of progress has been made in this direction, but new ideas and methods are still needed”.

Plan 2010

ELI-NP White-book, „Table 1: Overview of the main areas of the scientific case of ELI-NP” (p.7) as the first priority in Basic science:

- **Fundamental physics of perturbative and non-perturbative high-field QED: pair creation, high energy γ rays, birefringence of the quantum vacuum.**

Project: 5.3.1 “*Probing the Pair Creation from the Vacuum in the Focus of Strong Electrical Fields with a High Energy γ Beam*” R. Schützhold et al.

The experiments will allow for a new experimental window into the largely unexplored domain of non-perturbative quantum electrodynamics (QED). This has implications not just for QED, but also for fundamental issues in quantum field theory, as well as nuclear, atomic, plasma, gravitational and astro-physics.

Today

- **C. E. Turcu et al.** in the paper “*Quantum electrodynamics experiments with colliding petawatt laser pulses*” in High Power Laser Science and Engineering, Vol. 7, e10 (2019) **Now the 2 x 10 PW laser beams of the ELI-NP laser facility has the interaction chambers dedicated to QED experiments [42-44]**
- **M. Pentia et al.** “*Vacuum strong field QED interaction processes at ELI-NP facility*” in <https://arxiv.org/pdf/2307.09315.pdf> **Studies of fundamental QED processes possible to be investigated with high power lasers**

Tomorrow

Letter of Intent – Conceptual Design Report – Technical Design Report

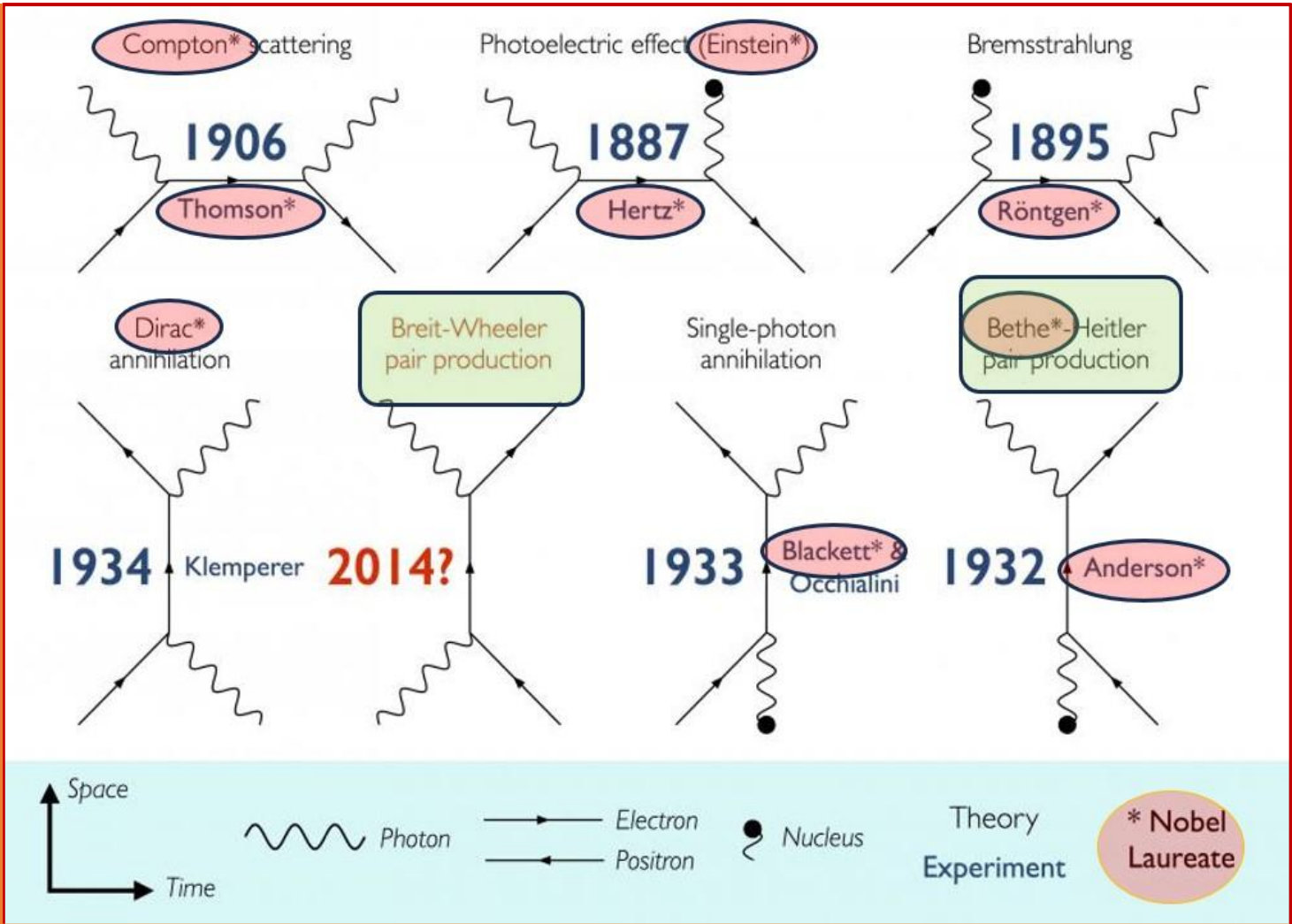
- Proposal of experimental works for measuring physical properties related to the production of e^+e^- pairs (Schwinger mechanism) in photon-multiphoton interaction (Breit-Wheeler), photon-electron or photon-nucleus (Bethe-Heitler) interaction and production and measurement of QED bound states (positronium).
- Experimental measurement of some fundamental QED processes with High Power Lasers at ELI-NP.

(conditioned by adequate funding for manpower, equipment and materials)

1.2 QED interaction processes – nowadays ones of the most interesting topics

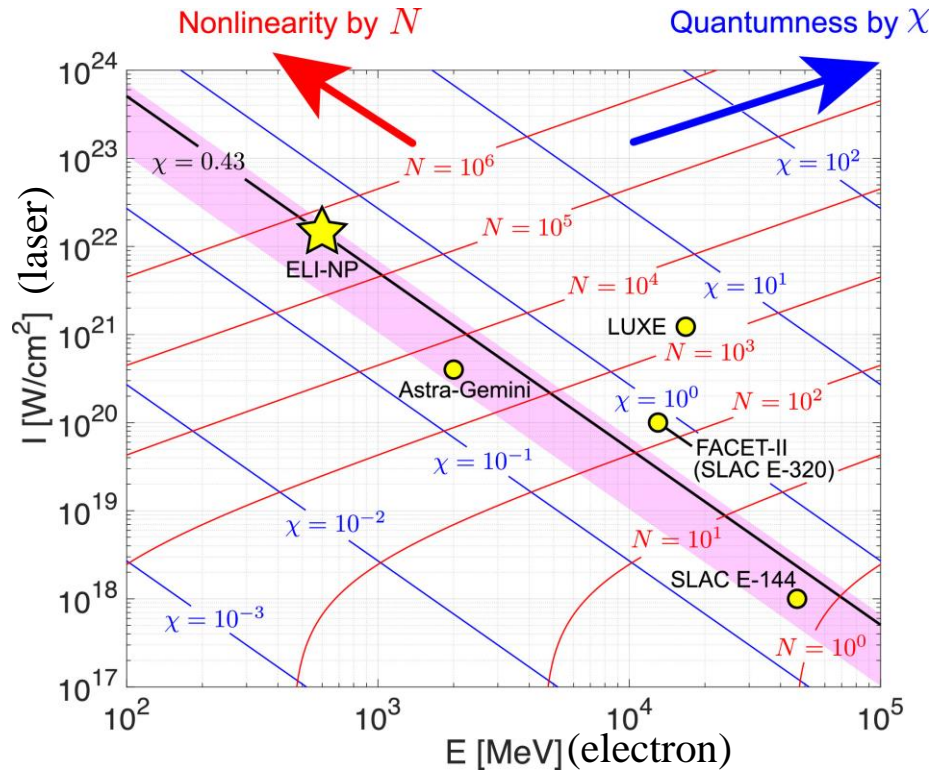
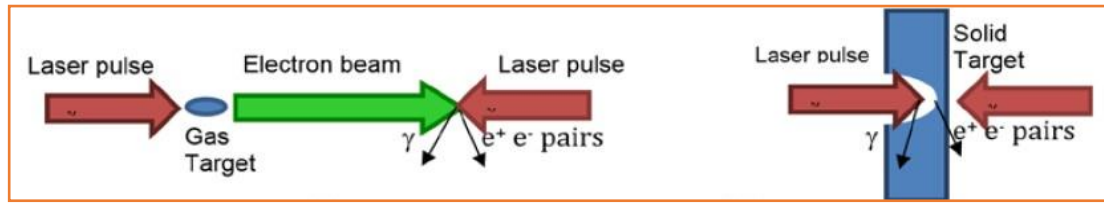
The Feynman diagrams for the QED light – matter interactions. Breit-Wheeler pair production has not yet been demonstrated experimentally.

<https://phys.org/news/2014-05-scientists-year-qest.html>
 credit O. J. Pike, F. Mackenroth, E. G. Hill and S. J Rose,
 “A photon-photon collider in a vacuum hohlraum”
Nature Photonics 8, 434-436 (2014).
 doi:10.1038/nphoton.2014.95



- The **ELI-ALPS laser** (Szeged - Hungary) will use the Heisenberg uncertainty relation $\Delta x \Delta p \geq \hbar/2$ to observe the evolving electron coordinates → instrumentalize the 2023 (Nobel prize) winner’s researches
- The **ELI-NP laser** (Magurele) will still use the same Heisenberg uncertainty relation $\Delta t \Delta E > \hbar/2$ to instrumentalize the light - matter conversion by **Breit-Wheeler and/or Bethe-Heitler pair production** with laser light

1.3 ELI-NP possibilities (K.Seto 2021)



Before collision (e + laser)

$$\begin{pmatrix} E \\ p \end{pmatrix} + N \times \begin{pmatrix} \hbar\omega \\ \hbar k \end{pmatrix} = \begin{pmatrix} E' \\ p' \end{pmatrix} + \begin{pmatrix} \hbar\omega' \\ \hbar k' \end{pmatrix}$$

After collision (e + gamma)

$$\chi \propto \hbar \times \text{electron energy } (E) \times \sqrt{\text{laser intensity } (I)}$$

$$N \propto \frac{\hbar\omega'}{E - \hbar\omega'} \times \frac{I}{E}, \quad \hbar\omega' = \frac{E}{2}$$

The physical regime diagram of RR. The curves at given N and χ are shown in the diagram. N is the number of absorbed laser photon and χ is intensity parameter. Here, an emitted photon energy $\hbar\omega'$ is selected as $\hbar\omega' = E/2$ for an electron energy E , $\theta_{in} = 155^\circ$ and $\hbar\omega = 1.5$ eV are taken into account to estimate where the proposed experiment at ELI-NP is. The pink ribbon represents the domain as $\chi \in [0.2, 0.5]$. We consider “linear” Compton scattering in the area where $N \leq 1$ (a single laser photon absorption) by given $\hbar\omega'$ and E . The star symbol shows the parameter set at ELI-NP. (K. Seto, Seminar 2021)

So, consider the uses of photons from 10 keV to GeV-class !
(K. Seto, Seminar 2021)

Outline

1. Introduction
2. Vacuum interactions – Schwinger effect
3. QED interaction processes (theory & exp.)
4. ELI-NP Experiments for SF-QED study
5. Physics of the QED processes at ELI-NP
6. Task Force, plan and resources

2.1 QED Vacuum fluctuation - Schwinger field E_{cr}

Under normal conditions, the physical vacuum, due to the quantum fluctuations, is in a permanent "boiling", with local production and annihilation of *virtual* particle-antiparticle pairs.

According to the Heisenberg principle, locally, on short time intervals Δt , there are energy fluctuations ΔE , so their product cannot be smaller than \hbar .

Then, on Δt time intervals, we have ΔE energy fluctuations that allow production of e^+e^- pairs:

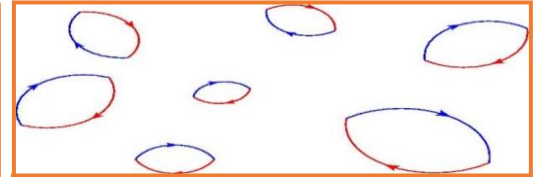
Locally on Δx space can be produced virtual electron-positron pairs, which live on the average Δt time, then they annihilate. A strong electric field can transfer enough energy to transform virtual pairs into real pairs.

The characteristic range $2\Delta x$ the electric field can produce e^+e^- pairs is given by *electron reduced Compton wavelength*

The virtual e^+e^- pair becomes a real one if a minimum energy W is transferred by the **electric field** E

or minimum value of the electric field is

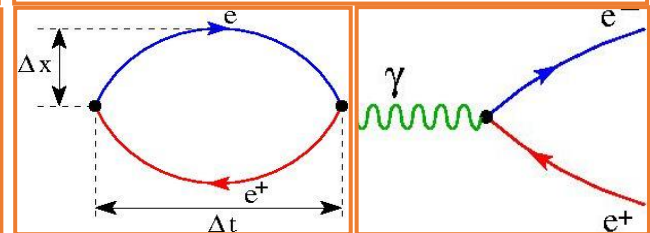
The critical value of the electric field E_{cr} (*Schwinger field*) i.e. starting value for spontaneously production of real e^+e^- pairs from laser field - vacuum interaction:



$$\Delta E \cdot \Delta t \geq \hbar$$

$$\begin{aligned} \hbar &= 1.054571817 \times 10^{-34} \text{ J} \cdot \text{s} \\ &= 6.582119569 \times 10^{-16} \text{ eV} \cdot \text{s} \end{aligned}$$

$$\begin{aligned} \Delta E &\approx 2m_e c^2 = 2 \cdot 0.511 \text{ MeV} \approx 10^6 \text{ eV} \\ \Delta t &\geq \hbar / 2m_e c^2 = 10^{-22} \text{ s} \end{aligned}$$



$$2\Delta x \approx 2c\Delta t = \frac{\hbar}{m_e c} = \lambda_c \approx 386 \cdot 10^{-15} \text{ m}$$

$$W = F \cdot \lambda = \frac{eE\hbar}{m_e c} > 2m_e c^2$$

$$E > \frac{2m_e^2 c^3}{\hbar e} = 2E_{cr}$$

$$E_{cr} = \frac{m_e^2 c^3}{\hbar e} = 1.323 \cdot 10^{18} \text{ V / m}$$

2.2 Pair creation from the vacuum - conversion of light to matter

One of the **amazing predictions of the QED** as a fundamental EM interaction, little studied experimentally, is the **conversion of light to matter**. Their nonperturbative and nonlinear features can shed a light on the properties of the **QED vacuum**.

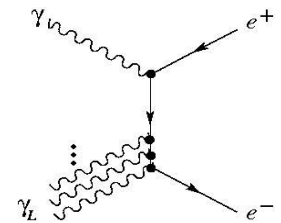
QED vacuum is a polarizable medium of virtual e^-e^+ pairs, they can be converted into real e^-e^+ pairs \rightarrow conversion to matter.

Such **particle creation from the EM field** is possible:

- in a static electric field – **Schwinger effect**,
- in a laser (coherent) photon field – **Breit-Wheeler production**, or
- in a combination of the two – **Bethe-Heitler production**,

has been of interest the crossover between the two pair production mechanisms:

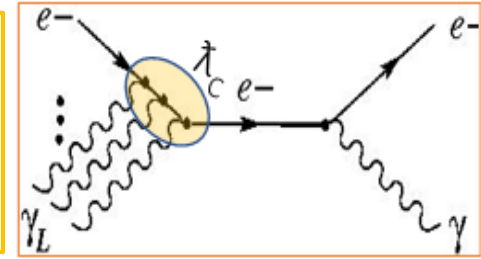
- **due to strong constant electric fields** but less than critical value $qEl < 2mc^2$ and
- **due to spatial or temporal variations** but less than critical value $\hbar\omega < 2mc^2$



Generation of Schwinger field at laser facility

2.3 Dimensionless Intensity classical parameter ξ

In a coherent multi-photon laser interaction, the constructive superposition of the electric field component ensures a total electric RMS field E_L close to the Schwinger critical field $E_{cr} = 1.323 \cdot 10^{18} \text{ V/m}$. This E_L value is higher the higher the photon density (laser intensity).



Laser intensity classical parameter ξ - the ratio of the laser field work on the electron Compton wavelength and the laser photon energy. Expresses the number of photons interacting over distance λ_c

$$\xi = \frac{eE_L \frac{\lambda_c}{\hbar\omega_L}}{m_e c \omega_L} = \frac{eE_L}{m_e c \omega_L} = eE_L \frac{\lambda_L}{m_e c^2} = \frac{m_e c^2}{\hbar\omega_L} \frac{E_L}{E_{cr}} \quad \text{where} \quad \lambda_c = \frac{\hbar}{m_e c} \quad \lambda_L = \frac{c}{\omega_L} \quad E_{cr} = \frac{m_e^2 c^3}{\hbar e}$$

When ξ is small the most probable are the processes with minimum possible number of photons.

At $\xi \ll 1$ the probabilities equals the perturbation (linear) theory probabilities and plane waves play a role of an individual photon.

At $\xi \sim 1$ or $\xi > 1$ the probabilities of absorbing different number of photons become comparable and the process becomes multiphoton, i.e., the probability has an essentially nonperturbative (nonlinear) dependence ξ on the field. Thus ξ is the **classical nonlinearity parameter**.

$\xi \gg 1$ with modern laser technology. The EM pulse with highest reported intensity had $\xi \approx 10^2$.

The ξ^2 measures laser intensity with $\langle E_L^2 \rangle$
as the field energy density of the laser beam

$$I_L = \varepsilon_0 c \langle E_L^2 \rangle \quad \Rightarrow \quad E_L = 1944 \cdot \sqrt{I_L}$$

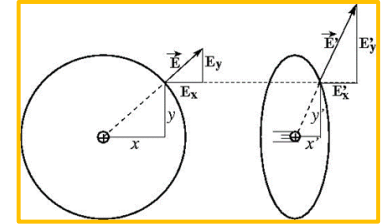
for ELI-NP intensity $I_L \approx 10^{22} - 10^{23} \text{ W/cm}^2$, laser light pulses lead to field intensity $E_L \approx 10^{14} - 10^{15} \text{ V/m}$

$$\xi^2 = 3.65 \times 10^{-19} I_L \lambda_L^2 \quad \text{for} \quad I_L \text{ in } \text{W/cm}^2 \text{ and } \lambda_L \text{ in } \mu\text{m}$$

At ELI-NP for wavelength $\lambda_L = 0.815 \mu\text{m}$ and pulse intensity $I_L \sim 10^{23} \text{ W/cm}^2$, we have $\xi \approx 500$

2.4 Dimensionless quantum nonlinearity parameter χ_e

E_L in the rest frame of a relativistic, counter-propagating electron with laboratory energy ε_e and Lorentz factor $\gamma_e = \varepsilon_e / mc^2 \gg 1$ the laser electric field strength appears **boosted** to $E^* = 2\gamma_e E_L$



for an electron beam energy $\varepsilon_e = 10$ GeV, the Lorentz factor is $\gamma_e = \varepsilon_e / m_e c^2 \approx 2 \cdot 10^4$ and if a laser beam collides it head-on, electron "sees" a boosted laser field $E^* \approx 2 \cdot 10^{18}$ V/m

Quantum nonlinearity parameter χ_e

$$\chi_e = 2\gamma_e \frac{E_L}{E_{cr}} = \frac{E^*}{E_{cr}}$$

Ratio of the laser RMS field E_L (in the e^- rest frame) E^* to the critical field E_{cr}

$$\gamma_e = \frac{\mathcal{E}_e}{m_e c^2} = \frac{e^- \text{ energy}}{e^- \text{ rest energy}}$$

$$\chi_e = 2\gamma_e \frac{E_L}{E_{cr}} = \left(2\gamma_e \frac{\hbar \omega_L}{m_e c^2} \right) \xi$$

Dimensionless quantum nonlinearity parameter (quantumness) χ_e connection with the intensity classical parameter ξ

χ_e accounts of the quantum nonlinear effect in $e-\gamma$ laser collision.

2.5 The critical value of the electric field E_{cr} (Schwinger field)

In conclusion:

Production of a strong EM field (Schwinger threshold) is done,

- by the coherent field superposition of intense laser beams, on the characteristic distance of the Compton wavelength. A laser beam has an electric (or magnetic) component proportional to its intensity. At ELI-NP with the intensity of $10^{22} - 10^{23}$ W/cm², we reach an electrical component of $10^{14} - 10^{15}$ V/m, nevertheless below the Schwinger critical value.

However, this ensures an important energy transfer to the electron, but insufficient to produce a high-energy photon that leads to the vacuum breakdown.

- The rest is obtained by the relativistic boost of the field in the electron rest system, by the Lorentz factor $\gamma_e = \epsilon_e / m_e c^2$.

For a 10 GeV electron, the electric field is amplified 20,000 times.

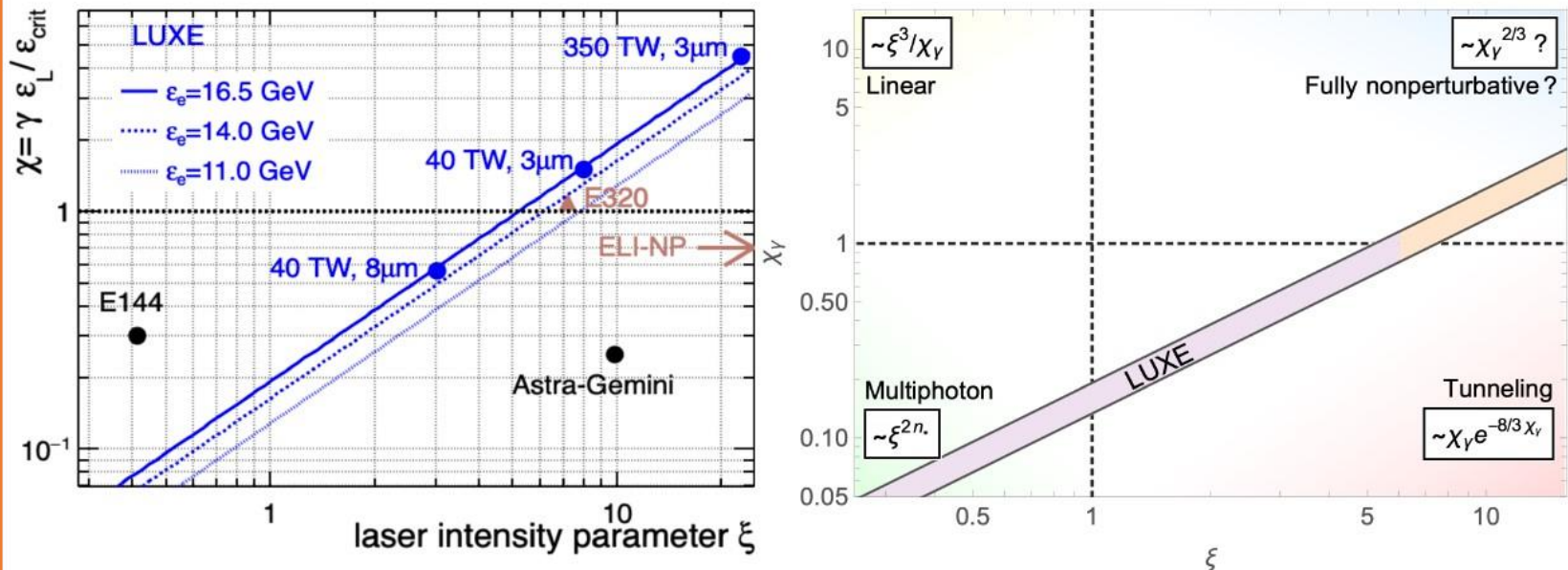
This way, the Schwinger critical field can be reached.

2.6 Parameter space for some SF-QED projects

LUXE

UCL

Strong-field QED parameter space



- E144: SLAC experiment in 1990s used 46.6 GeV electron beam.
 ➔ Values up to $\chi \sim 0.3$, $\xi \sim 0.4$, observed $e^- + n \gamma_L \rightarrow e^- + e^+ + e^-$ and power law.
- Astra-Gemini: laser-wake field experiment in RAL with ~ 1 GeV electrons.
- E320: new experiment at SLAC.
- **ELI-NP: in the future ...**
- LUXE: to cover broad parameter space and be the first to investigate high χ and high ξ . To measure collisions of real GeV photons and laser photons.

https://indico.desy.de/event/33338/contributions/117406/attachments/74703/95812/LUXE_PRC_May2022.pdf

Outline

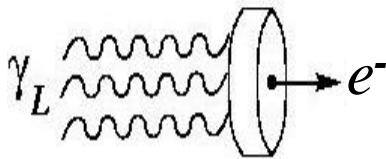
1. Introduction
2. Vacuum interactions – Schwinger effect
3. QED interaction processes (theory & exp.)
4. ELI-NP Experiments for SF-QED study
5. Physics of the QED processes at ELI-NP
6. Task Force, plan and resources

3.1 QED Processes - Conversion of Light to Matter

So far, the current theoretical and experimental works with high-power lasers have highlighted a series of QED processes and confirmed the possibility to approach them experimentally.

multi-photon
electron acceleration

Wakefield acceleration

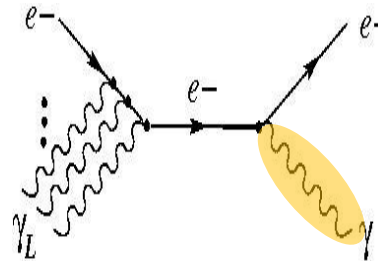


$$eE\ell < 2mc^2$$

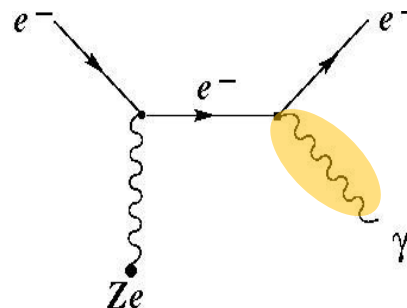
$$\hbar\omega < 2mc^2$$

multi-photon (or nuclear)
high-energy γ production

Inverse Compton scattering

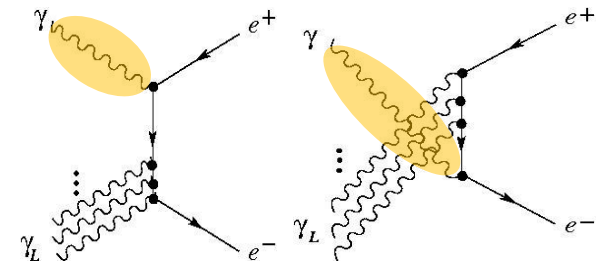


Bremsstrahlung

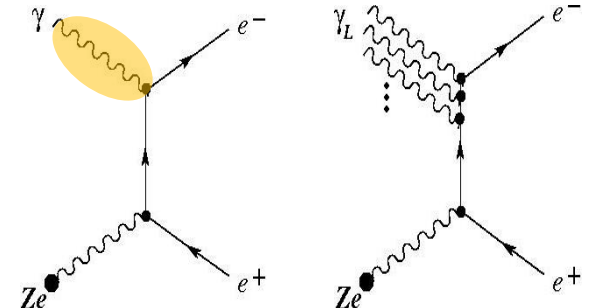


multi-photon (or nuclear)
 e^+e^- production

Breit-Wheeler pair production



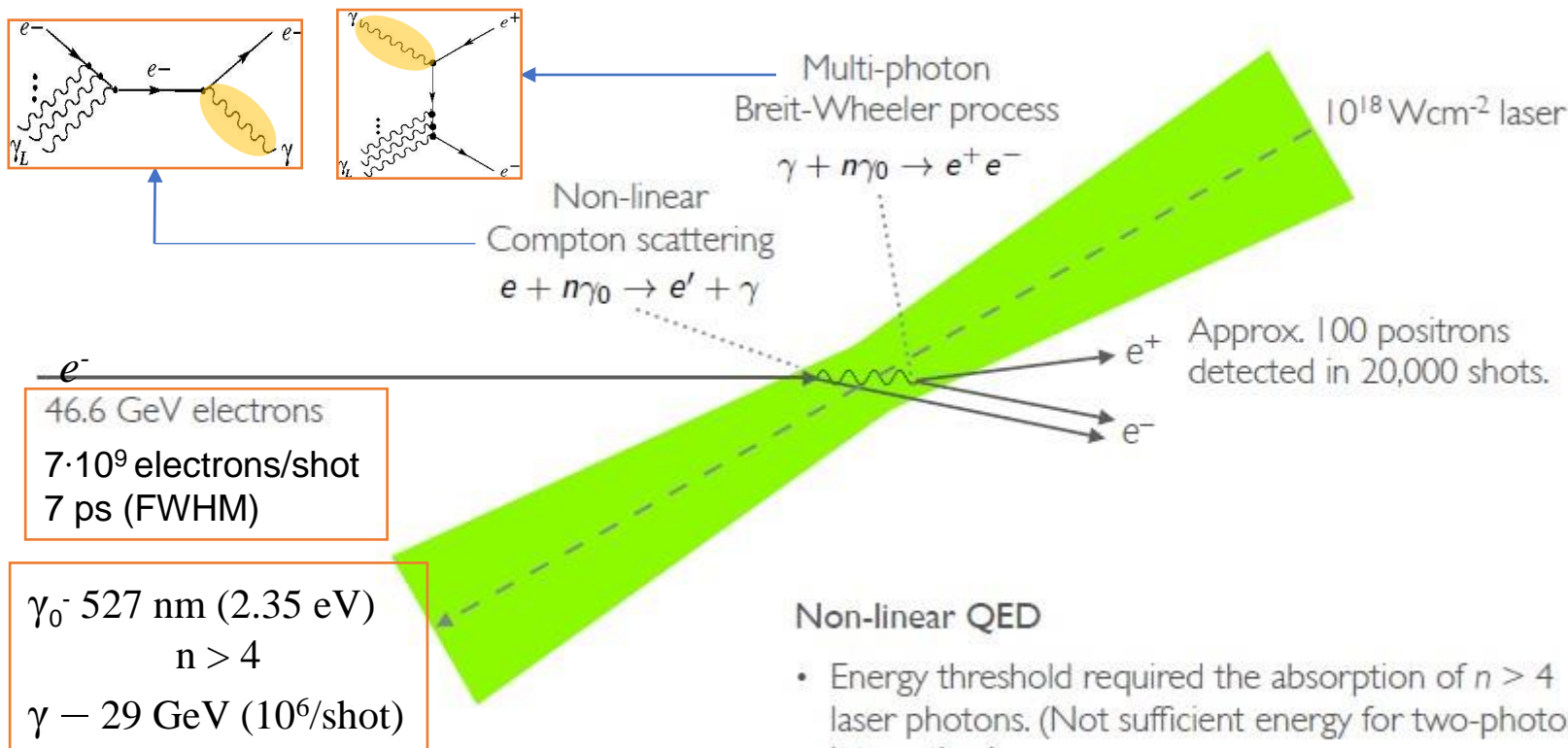
Bethe-Heitler pair production



First experimental confirmation

3.2 E-144 SLAC Experiment (electron – laser collision) - 1997

SLAC E-144 experiment:
first sign of positron production in light-by-light scattering



e^-
46.6 GeV electrons
 $7 \cdot 10^9$ electrons/shot
7 ps (FWHM)

γ_0 : 527 nm (2.35 eV)
 $n > 4$
 γ – 29 GeV (10^6 /shot)

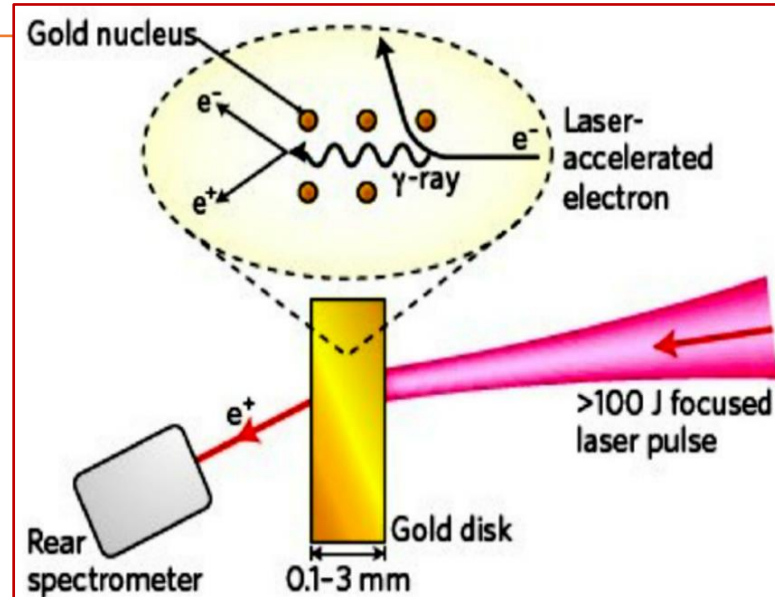
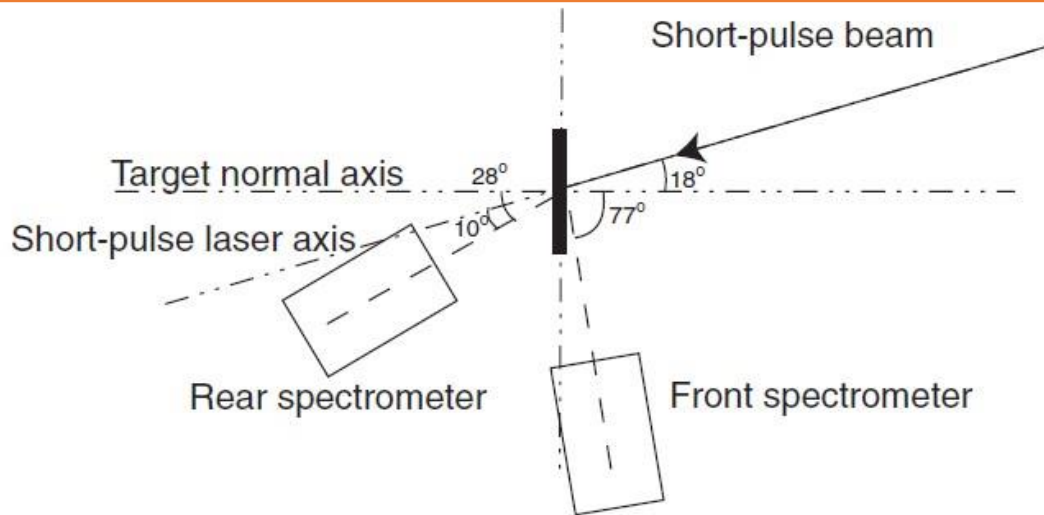
- Non-linear QED**
- Energy threshold required the absorption of $n > 4$ laser photons. (Not sufficient energy for two-photon interaction.)
 - Recently shown that, on average, $n = 6.44$ laser photons were absorbed.

Burke et al., PRL 79, 1626 (1997)
Hu & Müller, PRL 107, 090402 (2010)

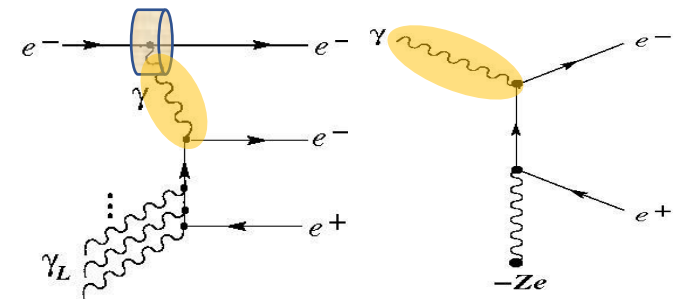
3.3 National Ignition Facility Experiment (2009)

So far, relatively simple experimental works have been done.

Hui Chen et al. in “*Relativistic Positron Creation Using Ultraintense Short Pulse Lasers*” **Phys. Rev. Lett.** **102(10)**, 105001 (2009) with the **Titan laser**, one of the two lasers in the **Jupiter facility** at the **National Ignition Facility (USA)**, with an energy of 250 J, by irradiating a high-Z target (Au ~1 mm) with laser pulses of 1054 nm, duration ~1 ps, intensity ~ 1×10^{20} W/cm² (see Fig.), 2×10^{10} positrons/sr were obtained, with energy < 20 MeV, with an anisotropic angular distribution, where the number of positrons recorded in the -77° direction being 10 times higher than the one on the 28° direction from the normal on the surface of the target.



Positrons are produced predominately by the **Bethe-Heitler process** and have an effective energy of 2–4 MeV, with the distribution peaking at 4–7 MeV. In this process the electrons, resulting from the interaction of the laser pulse with the target, produces bremsstrahlung gamma radiation of the order of MeV, which in turn, in the interaction with the electric field of the nucleus, generates electron-positron pairs. Such studies were further carried out with ultra-intense laser.



3.4 ELI-NP White Book - Scientific Case of ELI-NP (2010)

“The high power laser allows for intensities of up to 10^{24} W/cm². Here very interesting synergies are achievable with the γ beam and the brilliant high energy electron beam to study new fundamental processes in high field QED. When the γ beam is injected into the focus of the high intensity laser, which in this special case consists of a standing E-field of two focused lasers, *the most recent (2009) nonperturbative QED calculations predict that one can observe already at 10^{24} W/cm² the catalytic pair creation from the vacuum [2–4]. If confirmed, this would constitute a very basic non-perturbative textbook QED result.*”

Table 1: Overview of the main areas of the scientific case of ELI-NP

Science Case of ELI-NP	
Basic Science	Applications
<p>Fundamental physics of perturbative and non-perturbative high-field QED:</p> <ul style="list-style-type: none"> – pair creation, high energy γ rays, birefringence of the quantum vacuum 	<p>Developing nuclear resonance fluorescence (NRF) for nuclear materials and radioactive waste management:</p> <ul style="list-style-type: none"> – ^{235}U, ^{239}Pu, minor actinides, neutron poison
<p>High-resolution nuclear spectroscopy: (γ, γ'), (γ, n), (γ, p), (γ, α), (e, e'), $(e, e'\gamma)$, (γ, f)</p> <ul style="list-style-type: none"> – neutron halo isomers, chaotic properties of nuclear states, nuclear potential landscape, parity-violating meson-nucleon coupling, pygmy dipole resonance 	<p>Brilliant γ, X, n, e^+, e^- micro beams in material science and life science:</p> <ul style="list-style-type: none"> – (γ, n) reaction at threshold for low energy neutrons, (γ, e^+e^-) reaction at 2-3 MeV for cold positrons
<p>Astrophysics of the r-, s-, p-processes in nucleosynthesis:</p> <ul style="list-style-type: none"> – masses of waiting point nuclei, pygmy resonance 	<p>Developing techniques of laser acceleration and of a brilliant γ beam for nuclear physics:</p> <ul style="list-style-type: none"> – relativistic mirrors

Upcoming Experiments

3.5 Upcoming Experiments (ELI-NP competitors)

A. Gonoskov, T. G. Blackburn, and M. Marklund, S. S. Bulanov,

Charged particle motion and radiation in strong electromagnetic fields, Rev.Mod.Phys, V. 94, Oct - Dec 2022

<https://journals.aps.org/rmp/pdf/10.1103/RevModPhys.94.045001>

“Today experiments on radiation emission and pair creation in the strong-field regime form part of the planned experimental programs at almost every major petawatt or multi petawatt laser facility, including the

Extreme Light Infrastructure (ELI) (Weber et al., 2017; Gales et al., 2018)	Apollon (Papadopoulos et al., 2016)
Center for Relativistic Laser Science (CoReLS) (Yoon et al., 2021)	Station of Extreme Light - SEL (Cartlidge, 2018)
Omega Laser Facility (Rochester Univ.) (Bromage et al., 2019)	J-KAREN-P (Kiryama et al., 2020)
Zetawatt-Equivalent Ultrashort Pulse Laser System (ZEUS – Michigan Univ.) (Nees et al., 2020)	LUXE (Abramowicz et al, 2019; Meuren, 2019”

Name	Year	a_0^{\max}	χ^{\max}	Laser			e beam
				Power [TW]	A [μm^2]	λ [nm]	
E144	1990s	0.36	0.3	1	100	500 – 1000	$E_e = 46.6$ GeV, RF
Astra Gemini	2017	9.0	0.15 – 0.3	200	25	800 – 1000	$E_e \approx 1 - 2$ GeV LWFA
ELI-NP	2018	100	10	10000	10	800	up to 10 GeV, LWFA
FACET-II	2020	7.2	0.85	20	10	800	$E_e = 10$ GeV, RF
LUXE-I	2021	1.5	0.3	10	100	800	$E_e = 17.5$ GeV, RF
LUXE-II	2025	6.8	1.4	200	100	800	$E_e = 17.5$ GeV, RF

<https://arxiv.org/abs/1905.00059v1>

LUXE Workshop 2019, <https://arxiv.org/abs/1905.00059v1>

- M. Altarelli, et al "Probing strong-field QED in electron-photon interactions" in DESY, Hamburg, August 2018”

LUXE physics and SFQED Workshop, Sept. 2023, <https://conferences.weizmann.ac.il/SRitp/September2023/>

- Victor Malka, Gilad Perez, Noam Tal Hod, organizers, Weizmann Institute of Science.

LUXE competing project

3.6 LUXE (Laser Und XFEL Experiment) at DESY

<https://luxe.desy.de/>

launched nine years later then our proposal in ELI-NP White Book, published has:

- **Letter of Intent for the LUXE Experiment** (H. Abramowicz et al.) **2019**,
<https://arxiv.org/abs/1909.00860v1>
- **Conceptual Design Report for the LUXE Experiment** (H. Abramowicz, et al.) **2021**,
<https://arxiv.org/abs/2102.02032>
- **Technical Design Report for the LUXE Experiment** (H. Abramowicz, et al.) **2023**,
<https://arxiv.org/abs/2308.00515>

laser power to reach the Schwinger field ($\chi \sim 1$)

- non-relativistic photons : $I = 2 \cdot 10^{29}$ W/cm² (beyond currently achievable values)
- EU-XFEL: $E_\gamma \approx 10$ GeV: $I = 10^{20}$ W/cm² (well-tested laser technology)
- ELI-NP: $E_\gamma \approx 1$ GeV: $I = 10^{22}$ W/cm² (state-of-the-art laser needed)

G. Grzelak, LUXE slides, 2020

https://indico.cern.ch/event/882870/contributions/3720001/attachments/1974963/3286730/The_LUXE_GG_Seminar.pdf

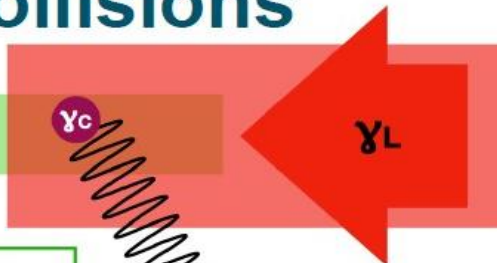
- E144: SLAC experiment in 1990s used 46.6 GeV electron beam.
 ➔ Values up to $\chi \sim 0.3$, $\xi \sim 0.4$, observed $e^- + n \gamma_L \rightarrow e^- + e^+ + e^-$ and power law.
- Astra-Gemini: laser-wake field experiment in RAL with ~ 1 GeV electrons.
- E320: new experiment at SLAC.
- ELI-NP: in the future ...
- LUXE: to cover broad parameter space and be the first to investigate high χ and high ξ .
To measure collisions of real GeV photons and laser photons.

Wing (LUXE) slides, 2022

https://indico.desy.de/event/33338/contributions/117406/attachments/74703/95812/LUXE_PRC_May2022.pdf

LUXE: electron-laser collisions

High-energy electrons
(16.5 GeV XFEL beam)



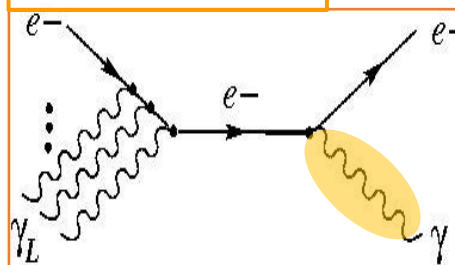
High-intensity LASER
(Tera-Watt, 800nm)
→ large E-field

note: in reality, LASER
crossing angle $\theta=17.2^\circ$

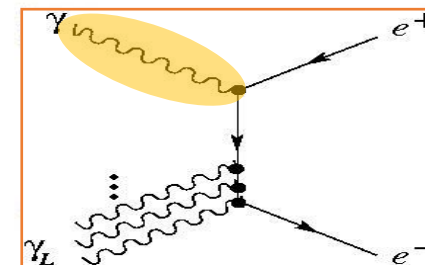
Lorentz boost:
electrons “see” larger
E-field of the LASER
in their rest frame:
 $E^* = \gamma_e \mathcal{E}_L (1 + \cos \theta)$

**electron-positron
pair production**

Inverse Compton



+



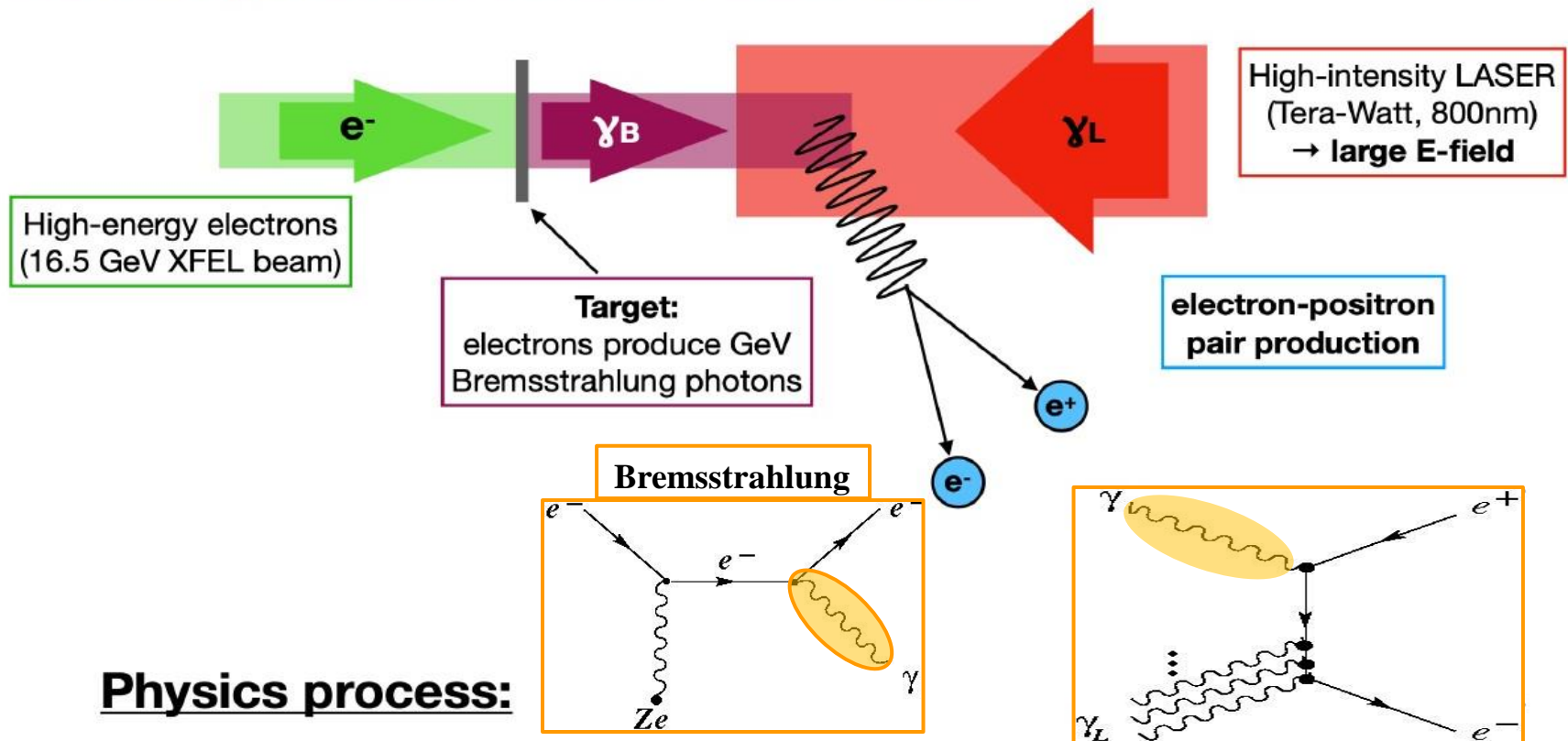
Physics processes:

- 1 **Non-linear Compton Scattering:** $e^- + n\gamma_L \rightarrow e^- + \gamma_C$
- 2 **Non-linear Breit-Wheeler pair production:** $\gamma_C + n\gamma_L \rightarrow e^+ + e^-$

• LUXE main goals:

- ➔ Measure Compton scattering (and edge position) versus laser intensity.
- ➔ Measure positron rate versus laser intensity.

LUXE: photon-laser collisions



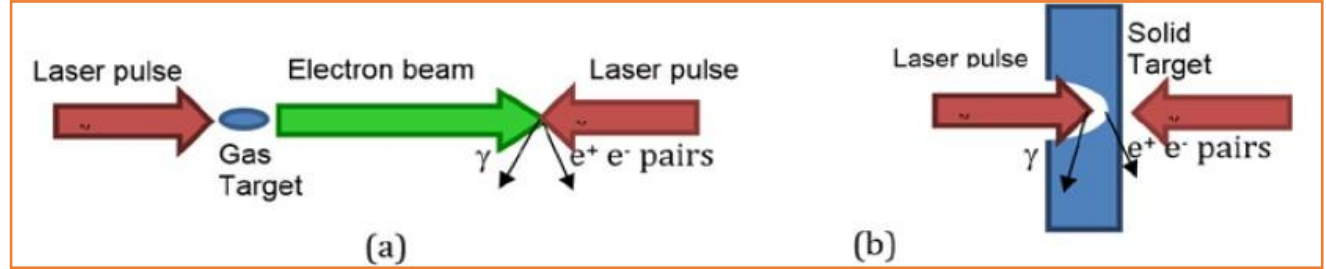
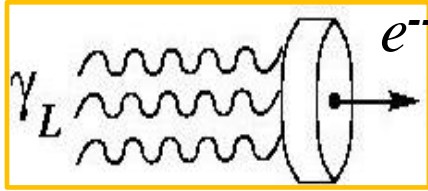
Non-linear Breit-Wheeler pair production : $\gamma_B + n\gamma_L \rightarrow e^+ + e^-$

Outline

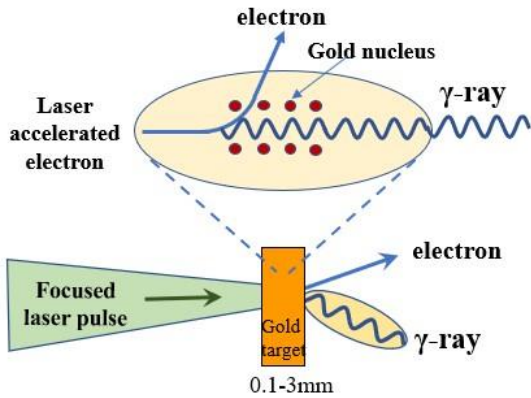
1. Introduction
2. Vacuum interactions – Schwinger effect
3. QED interaction processes (theory & exp.)
4. ELI-NP Experiments for SF-QED study
5. Physics of the QED processes at ELI-NP
6. Task Force, plan and resources

4.1 Particular interest - multiphoton Breit-Wheeler pair production

Wakefield acceleration

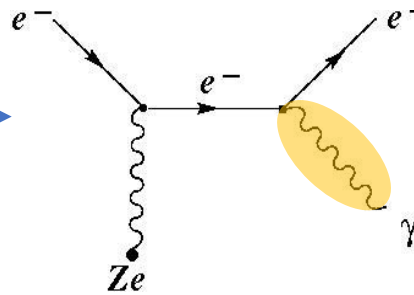


Bremsstrahlung



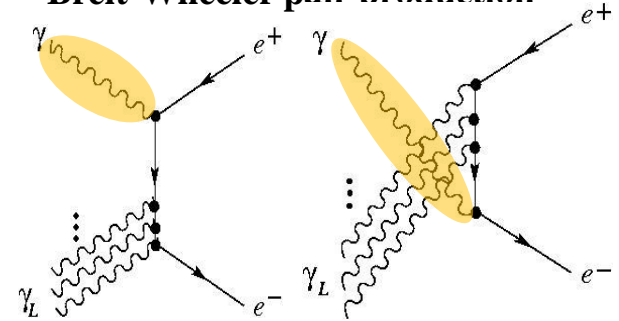
GeV γ sources

Bremsstrahlung

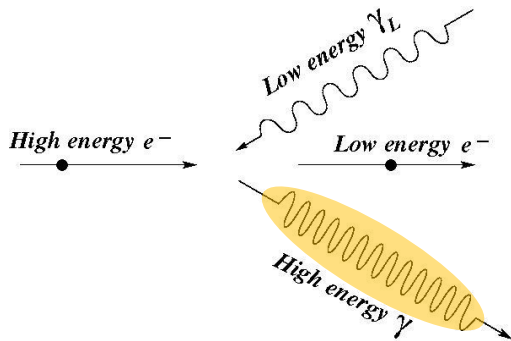


Pair production

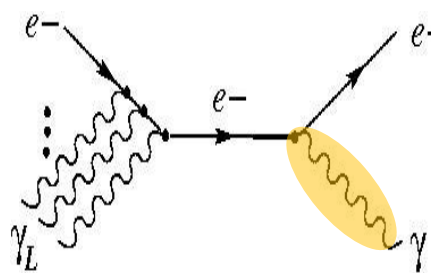
Breit-Wheeler pair production



Inverse Compton scattering

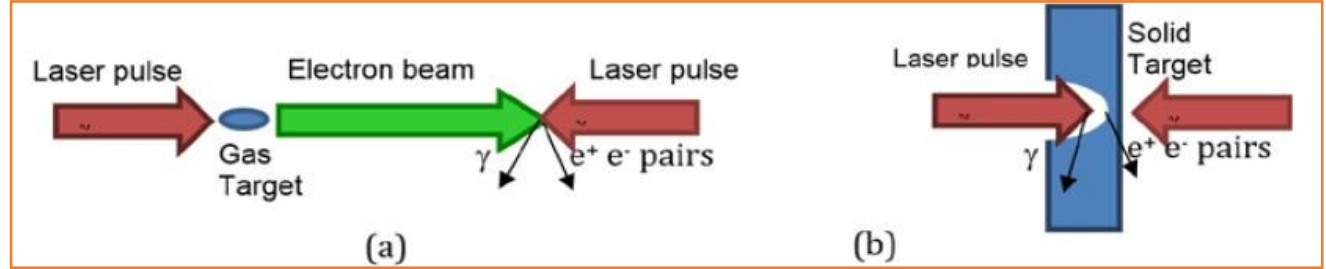
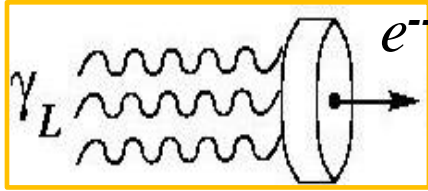


Inverse Compton scattering

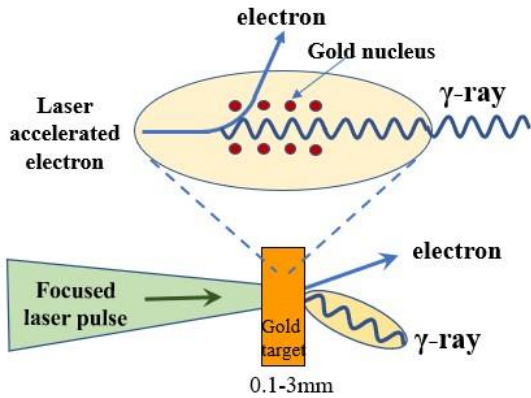


4.2 Particular interest - multiphoton Bethe-Heitler pair production

Wakefield acceleration

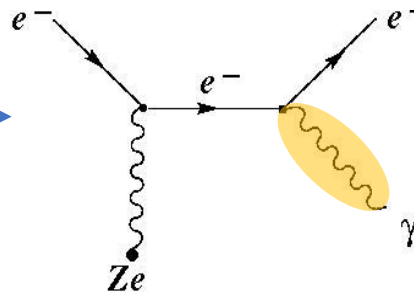


Bremsstrahlung



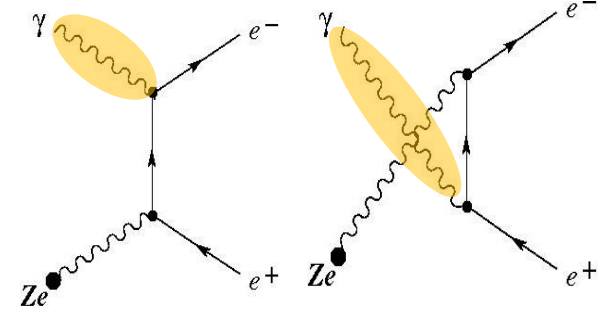
GeV γ sources

Bremsstrahlung

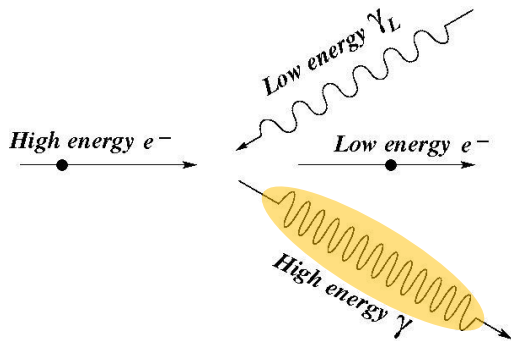


Pair production

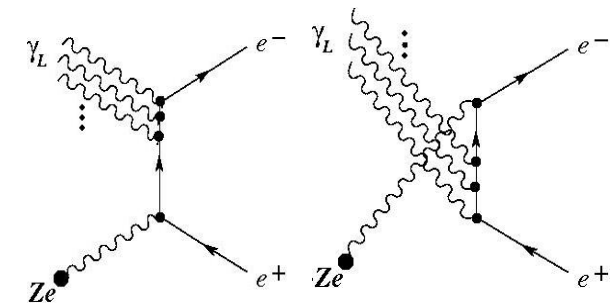
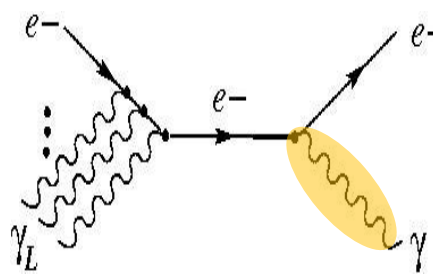
Bethe-Heitler pair production



Inverse Compton scattering



Inverse Compton scattering



4.3 ELI-NP Experimental area for SF-QED Study

I.C.E. Turcu et al, “High field physics and QED experiments at ELI-NP”, Rom. Rep. Phys. 68, Supplement, S145 (2016).

The experimental area E6 at ELI-NP is ready for investigating high field physics and QED for production of electron-positron-pairs and of energetic gamma-rays.

Two pump-probe colliding 10 PW laser beams are proposed for the E6 interaction chamber. The focused pump laser beam accelerates the electrons to relativistic energies. The accelerated electron bunches interact with the very high EM field of the focused probe laser beam.

Proposed two main types of experiments with: (a) *gas targets* in which the pump laser-beam is focused by a long focal length mirror and drives a wakefield in which the electron bunch is accelerated to multi-GeV energies and then exposed to the EM field of the probe laser which is tightly focused; (b) *solid targets* in which both the pump and probe laser beams are focused on the solid target, one accelerating the electrons in the solid and the other, delayed, providing the high electric field to which the relativistic electrons are subjected.

We propose to use the unique capabilities of ELI-NP to:

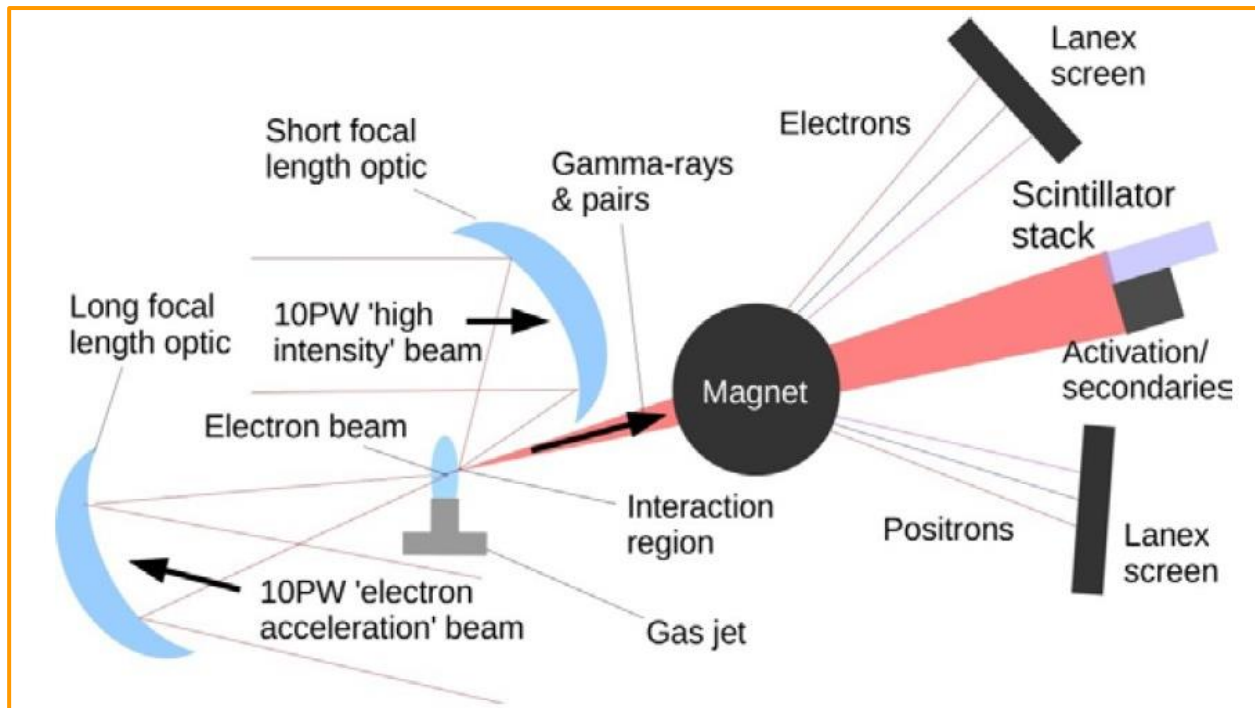
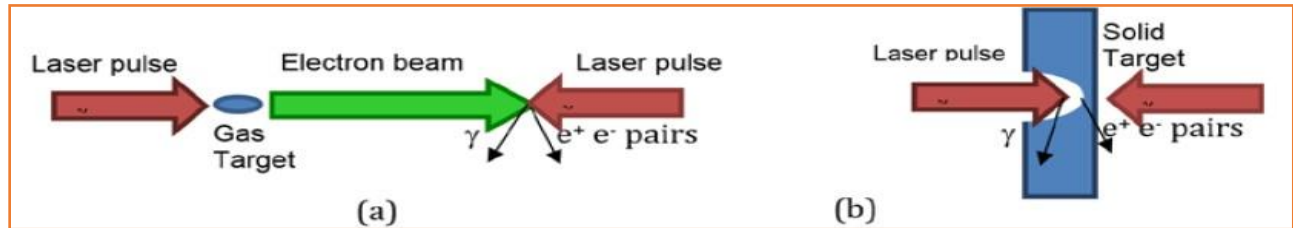
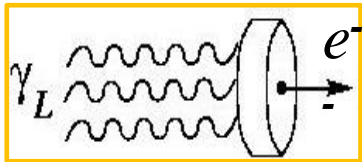
1. Observe the transition to the very **nonlinear Compton scattering** regime,
2. Measure the **nonlinear Breit-Wheeler pair production**.
3. Measure the **nonlinear Bethe-Heitler pair production** (nuclear physics)

4.4 Setup for SF-QED study

I.C.E. Turcu et al, "High field physics and QED experiments at ELI-NP", Rom. Rep. Phys. 68, Supplement, S145 (2016).

- ELI-NP facility will enable for the first time the use of two 10 PW laser beams for QED experiments.
- The first beam will accelerate electrons to relativistic energies.
- The second beam will subject relativistic electrons to the strong electromagnetic field generating QED processes: intense gamma ray radiation and electron-positron pair formation.

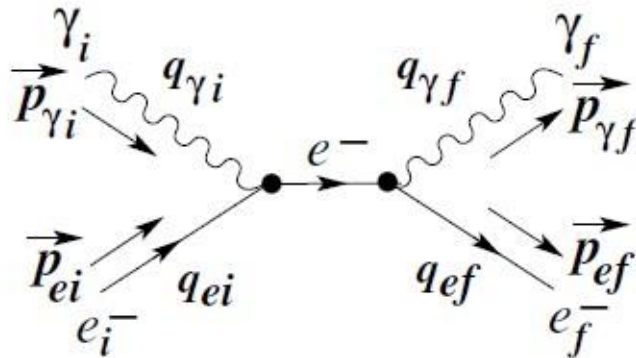
Wakefield acceleration



Outline

1. Introduction
2. Vacuum interactions – Schwinger effect
3. QED interaction processes (theory & exp.)
4. ELI-NP Experiments for SF-QED study
5. Physics of the QED processes at ELI-NP
6. Task Force, plan and resources

5.1 Kinematics of the γ - e scattering

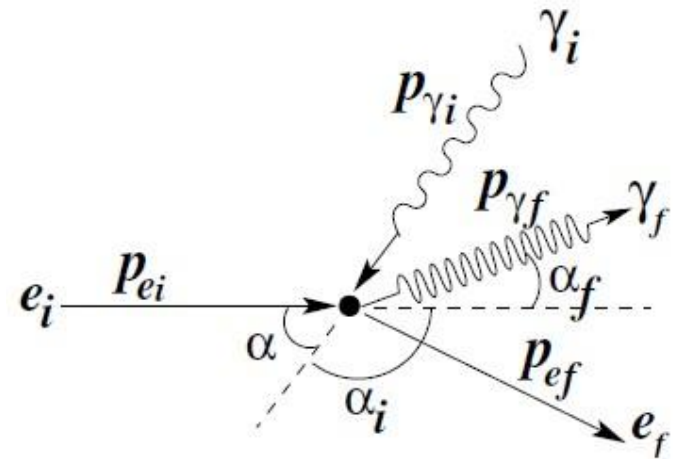


Kinematics of the $e_i \gamma_i \rightarrow e_f \gamma_f$ scattering

The 4-momentum conservation, see Fig.

$$q_{\gamma i} + q_{e i} = q_{\gamma f} + q_{e f}$$

$$\begin{aligned} \epsilon_\gamma &= \hbar \omega & \vec{p}_\gamma &= \frac{\epsilon_\gamma}{c} \vec{n}_\gamma \\ \epsilon_e &= \gamma_e m_e c^2 & \vec{p}_e &= \gamma_e m_e \vec{v}_e = \frac{\epsilon_e}{c^2} \vec{v}_e = \frac{\epsilon_e}{c} \vec{\beta}_e \\ q &\equiv \left(\frac{E}{c}, \vec{p} \right) & \text{metric: } g_{\mu\mu} &= (1, -1, -1, -1) \\ q^2 &= \frac{E^2}{c^2} - \vec{p}^2 = m_e^2 c^2 \end{aligned}$$



$q_{\gamma i} = \frac{\epsilon_{\gamma i}}{c} \left(1, \vec{n}_{\gamma i} \right)$	$q_{\gamma f} = \frac{\epsilon_{\gamma f}}{c} \left(1, \vec{n}_{\gamma f} \right)$	$\beta_e = \frac{p_e c}{\epsilon_e} = \frac{v_e}{c}$
$q_{e i} = \frac{\epsilon_{e i}}{c} \left(1, \vec{\beta}_{e i} \right)$	$q_{e f} = \frac{\epsilon_{e f}}{c} \left(1, \vec{\beta}_{e f} \right)$	$\gamma_e = \frac{\epsilon_e}{m_e c^2} = \frac{1}{\sqrt{1 - \beta_e^2}}$

$$\epsilon_{\gamma f} = \frac{\epsilon_{e i}}{1 + \frac{m_e^2 c^4}{\epsilon_{\gamma i} \epsilon_{e i}} \frac{1}{(1 + \beta_{e i} \cos \alpha)}}$$

5.2 Feynman Diagrams QED Processes

PROCES	INTERACTIA	ELEMENT MATRICE \hat{S}
Imprăștiere foton-electron $\gamma + e^- \rightarrow \gamma + e^-$ Imprăștiere foton-pozitron $\gamma + e^+ \rightarrow \gamma + e^+$		$\langle \gamma, e^- \hat{S} \gamma, e^- \rangle$ $\langle \gamma, e^+ \hat{S} \gamma, e^+ \rangle$
Anihilare perechi e^+e^- $e^- + e^+ \rightarrow \gamma + \gamma$		$\langle \gamma, \gamma \hat{S} e^-, e^+ \rangle$
Producere perechi e^+e^- $\gamma + \gamma \rightarrow e^- + e^+$		$\langle e^-, e^+ \hat{S} \gamma, \gamma \rangle$
Imprăștierea Møller e^- $e^- + e^- \rightarrow e^- + e^-$ Imprăștierea Møller e^+ $e^+ + e^+ \rightarrow e^+ + e^+$		$\langle e^-, e^- \hat{S} e^-, e^- \rangle$ $\langle e^+, e^+ \hat{S} e^+, e^+ \rangle$

PROCES	INTERACTIA	ELEMENT MATRICE \hat{S}
Imprăștierea Bhabha $e^- + e^+ \rightarrow e^- + e^+$		$\langle e^-, e^+ \hat{S} e^-, e^+ \rangle$
Energie proprie electron $e^- \rightarrow e^-$ Energie proprie pozitron $e^+ \rightarrow e^+$		$\langle e^- \hat{S} e^- \rangle$ $\langle e^+ \hat{S} e^+ \rangle$
Energie proprie foton $\gamma \rightarrow \gamma$		$\langle \gamma \hat{S} \gamma \rangle$
Energie vacuum Vacuum \rightarrow Vacuum		$\langle 0 \hat{S} 0 \rangle$

$$\left\{ \begin{aligned}
 \hat{A}_\mu(x) &= \int \frac{d^3\vec{k}}{(2\pi)^3} \frac{1}{2\omega} \left[\underbrace{\hat{a}_\lambda(\vec{k}) \epsilon_\mu^\lambda e^{-ik \cdot x}}_{\sim \hat{A}_\mu^-(x)} + \underbrace{\hat{a}_\lambda^\dagger(\vec{k}) \epsilon_\mu^\lambda e^{ik \cdot x}}_{\sim \hat{A}_\mu^+(x)} \right] \\
 \hat{\psi}(x) &= \int \frac{d^3\vec{p}}{(2\pi)^3} \frac{m}{\omega} \left[\underbrace{\hat{b}(\vec{p}) u(\vec{p}) e^{-ip \cdot x}}_{\sim \hat{\psi}^-(x)} + \underbrace{\hat{c}^\dagger(\vec{p}) v(\vec{p}) e^{ip \cdot x}}_{\sim \hat{\psi}^+(x)} \right] \\
 \hat{\bar{\psi}}(x) &= \int \frac{d^3\vec{p}}{(2\pi)^3} \frac{m}{\omega} \left[\underbrace{\hat{c}(\vec{p}) \bar{v}(\vec{p}) e^{-ip \cdot x}}_{\sim \hat{\bar{\psi}}^-(x)} + \underbrace{\hat{b}^\dagger(\vec{p}) \bar{u}(\vec{p}) e^{ip \cdot x}}_{\sim \hat{\bar{\psi}}^+(x)} \right]
 \end{aligned} \right.$$

$\hat{A}_\mu^-(x) \rightarrow \hat{a}$ - anihilare foton în x

$\hat{A}_\mu^+(x) \rightarrow \hat{a}^\dagger$ - creare foton în x

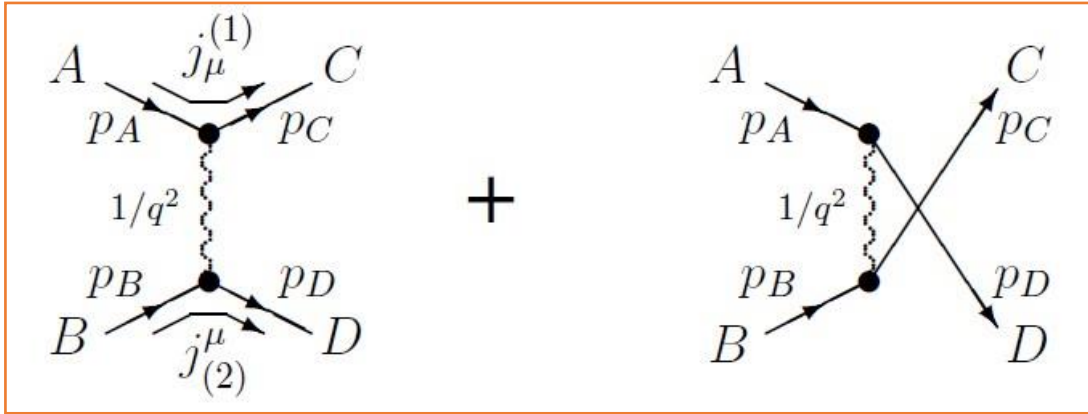
$\hat{\psi}^-(x) \rightarrow \hat{b}$ - anihilare electron în x

$\hat{\psi}^+(x) \rightarrow \hat{c}^\dagger$ - creare pozitron în x

$\hat{\bar{\psi}}^-(x) \rightarrow \hat{c}$ - anihilare pozitron în x

$\hat{\bar{\psi}}^+(x) \rightarrow \hat{b}^\dagger$ - creare electron în x

5.3 Cross section evaluation (example - Moller e^-e^- Scattering)



$$\left. \frac{d\sigma}{d\Omega} \right|_{scm} = \frac{1}{64\pi^2 s} \frac{|\vec{p}_f|}{|\vec{p}_i|} |\mathcal{M}|^2$$

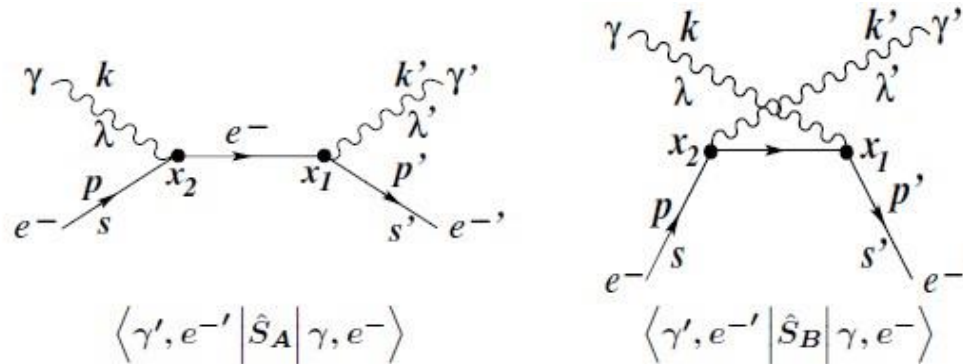
$$-i\mathcal{M} = \left(i e \bar{u}_C \gamma^\mu u_A \right) \left(\frac{-i g_{\mu\nu}}{q^2} \right) \left(i e \bar{u}_D \gamma^\nu u_B \right)$$

$$\mathcal{M} = -e^2 \frac{(\bar{u}_C \gamma_\mu u_A)(\bar{u}_D \gamma^\mu u_B)}{(p_C - p_A)^2} + e^2 \frac{(\bar{u}_D \gamma_\mu u_A)(\bar{u}_C \gamma^\mu u_B)}{(p_D - p_A)^2}$$

$$|\mathcal{M}|^2 \longrightarrow \overline{|\mathcal{M}|^2} \equiv \frac{1}{(2s_A + 1)(2s_B + 1)} \sum_{\text{toate stările de spin}} |\mathcal{M}|^2$$

$$\left. \frac{d\sigma}{d\Omega} \right|_{scm} = \frac{1}{64\pi^2 s} \frac{|\vec{p}_f|}{|\vec{p}_i|} \overline{|\mathcal{M}|^2} = \frac{m^2 c^4 \alpha^2}{16p^4} \left(\frac{1}{\sin^4 \frac{\theta}{2}} + \frac{1}{\cos^4 \frac{\theta}{2}} - \frac{1}{\sin^2 \frac{\theta}{2} \cos^2 \frac{\theta}{2}} \right)$$

5.4 Evaluation Feynman Diagrams: $\gamma - e^-$ scattering



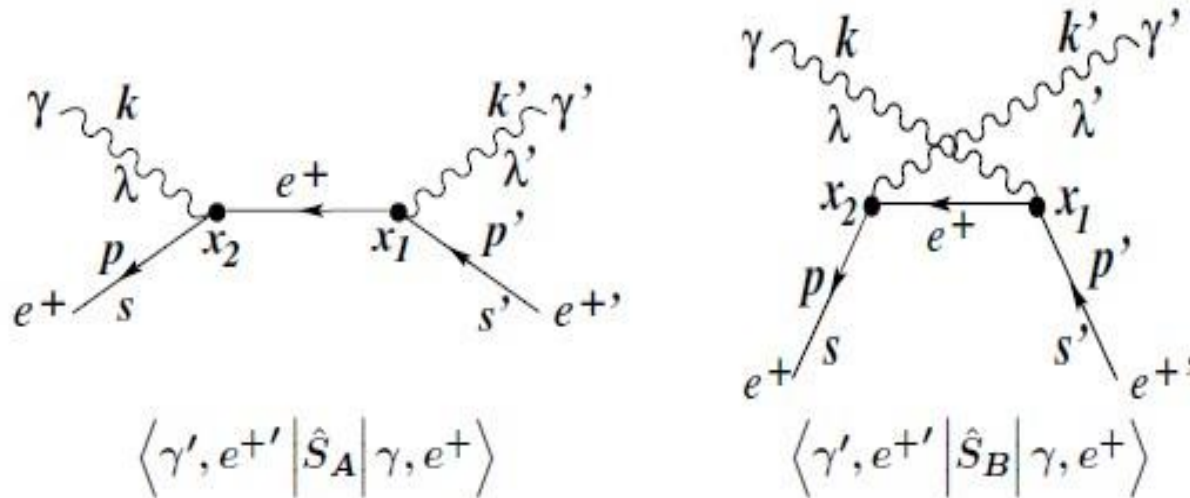
- Folosind componentele corespunzătoare de creare/anihilare din $\hat{\psi}(x)$, $\hat{\bar{\psi}}(x)$ și $\hat{A}_\mu(x)$

$$\begin{aligned}
 \hat{S}_A &= -e^2 \int d^4x_1 d^4x_2 N \left[\begin{array}{cccccc}
 \text{crea.} & \text{crea.} & & & \text{anih.} & \text{anih.} \\
 e^{-'} & \gamma' & & & \gamma & e^- \\
 \downarrow & \downarrow & & & \downarrow & \downarrow \\
 (\hat{\bar{\psi}}_{x_1}^+) & (\hat{A}_{x_1}^+) & \underbrace{(\hat{\psi}_{x_1}^-)(\hat{\psi}_{x_2}^+)}_{iS_F(x_1-x_2)} & (\hat{A}_{x_2}^-) & (\hat{\psi}_{x_2}^-) &
 \end{array} \right] \\
 \hat{S}_B &= -e^2 \int d^4x_1 d^4x_2 N \left[\begin{array}{cccccc}
 \text{crea.} & \text{crea.} & & & \text{anih.} & \text{anih.} \\
 e^{-'} & \gamma' & & & \gamma & e^- \\
 \downarrow & \downarrow & & & \downarrow & \downarrow \\
 (\hat{\bar{\psi}}_{x_1}^+) & (\hat{A}_{x_2}^+) & \underbrace{(\hat{\psi}_{x_1}^-)(\hat{\psi}_{x_2}^+)}_{iS_F(x_1-x_2)} & (\hat{A}_{x_1}^-) & (\hat{\psi}_{x_2}^-) &
 \end{array} \right]
 \end{aligned}$$

$$\langle \gamma', e^{-'} | \hat{S}_{ge}^{(2)} | \gamma, e^- \rangle = (2\pi)^4 \delta^4(p+k-p'-k') \mathcal{M}_{fi}$$

$$\left\{ \begin{array}{l}
 \mathcal{M}_{fi} = \mathcal{M}_{fi}^A + \mathcal{M}_{fi}^B \\
 \mathcal{M}_{fi}^A = -e^2 \bar{u}_{s'p'} \not{\epsilon}_{\lambda'} iS_F(p+k) \not{\epsilon}_\lambda u_{s\bar{p}} \\
 \mathcal{M}_{fi}^B = -e^2 \bar{u}_{s'p'} \not{\epsilon}_{\lambda'} iS_F(p-k') \not{\epsilon}_\lambda u_{s\bar{p}}
 \end{array} \right.$$

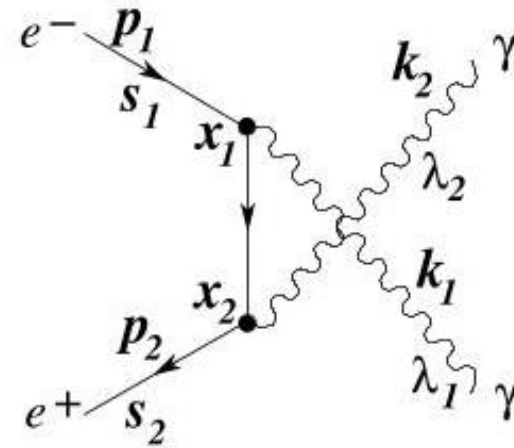
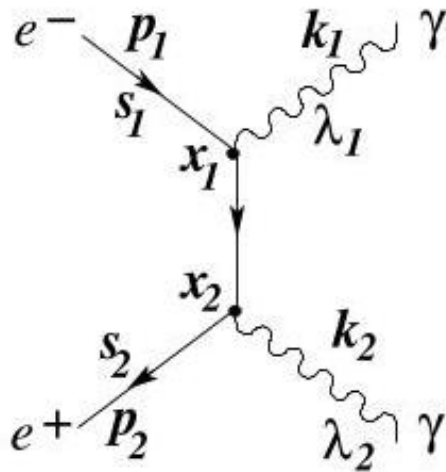
5.5 Evaluation Feynman Diagrams: $\gamma - e^+$ scattering



- Folosind componentele corespunzătoare de creare/anihilare din $\hat{\psi}(x)$, $\hat{\bar{\psi}}(x)$ și $\hat{A}_\mu(x)$

$$\begin{aligned}
 \langle f | \hat{S}_A | i \rangle &= -e^2 \int d^4x_1 d^4x_2 N \left[\overset{\text{crea.}}{e^{+'}} \downarrow \left(\hat{\psi}_{x_1}^+ \right) \overset{\text{crea.}}{\gamma'} \downarrow \left(\hat{A}_{x_1}^+ \right) \underbrace{\left(\hat{\psi}_{x_1}^- \right) \left(\hat{\bar{\psi}}_{x_2}^+ \right)}_{iS_F(x_1-x_2)} \overset{\text{anih.}}{\gamma} \downarrow \left(\hat{A}_{x_2}^- \right) \overset{\text{anih.}}{e^+} \downarrow \left(\hat{\bar{\psi}}_{x_2}^- \right) \right] \\
 \langle f | \hat{S}_B | i \rangle &= -e^2 \int d^4x_1 d^4x_2 N \left[\overset{\text{crea.}}{e^{+'}} \downarrow \left(\hat{\psi}_{x_1}^+ \right) \overset{\text{crea.}}{\gamma'} \downarrow \left(\hat{A}_{x_2}^+ \right) \underbrace{\left(\hat{\psi}_{x_1}^- \right) \left(\hat{\bar{\psi}}_{x_2}^+ \right)}_{iS_F(x_1-x_2)} \overset{\text{anih.}}{\gamma} \downarrow \left(\hat{A}_{x_1}^- \right) \overset{\text{anih.}}{e^+} \downarrow \left(\hat{\bar{\psi}}_{x_2}^- \right) \right]
 \end{aligned}$$

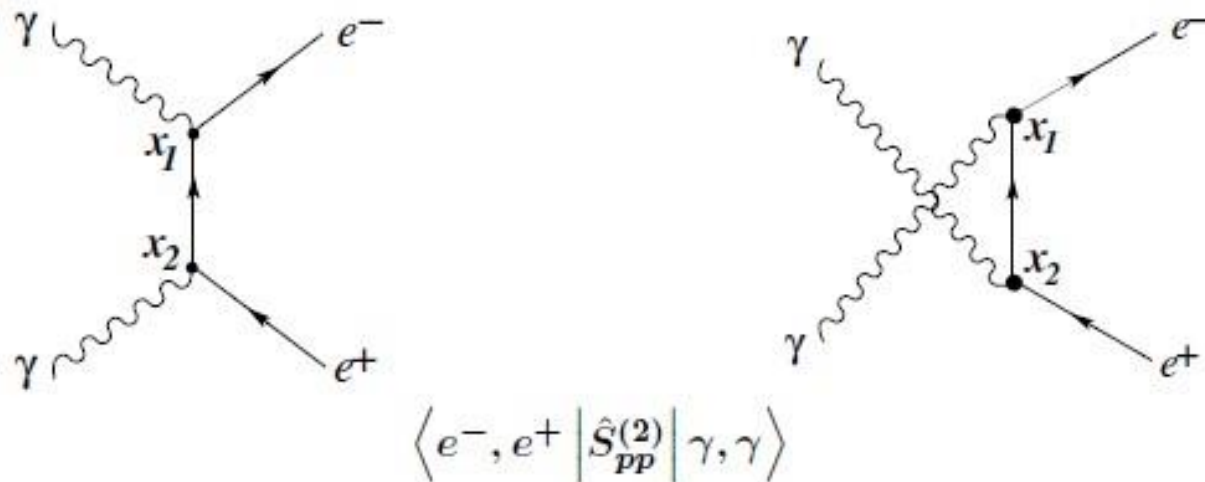
5.6 Evaluation Feynman Diagrams Pair Annihilation: $e^-e^+ \rightarrow \gamma\gamma$



- Folosind componentele corespunzătoare de creare/anihilare din $\hat{\psi}(x)$, $\hat{\bar{\psi}}(x)$ și $\hat{A}_\mu(x)$

$$\hat{S}_{ap}^{(2)} = -e^2 \int d^4x_1 d^4x_2 N \left[\begin{array}{cccccc} \text{anih.} & \text{crea.} & & & \text{crea.} & \text{anih.} \\ e^- & \gamma & & & \gamma & e^+ \\ \downarrow & \downarrow & & & \downarrow & \downarrow \\ (\hat{\psi}_{x_1}^-) & (\hat{A}_{x_1}^+) & \underbrace{(\hat{\psi}_{x_1}^-) (\hat{\psi}_{x_2}^+)}_{iS_F(x_1-x_2)} & & (\hat{A}_{x_2}^+) & (\hat{\psi}_{x_2}^-) \end{array} \right]$$

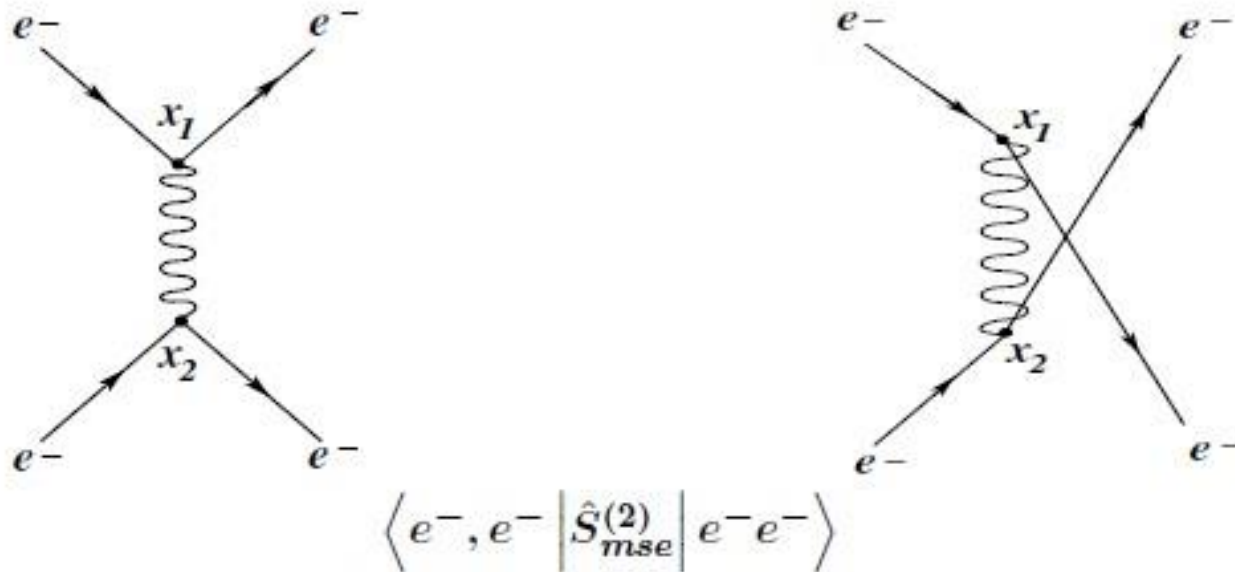
5.7 Evaluation Feynman Diagrams Pair Production (Breit-Wheeler): $\gamma\gamma \rightarrow e^-e^+$



- Folosind componentele corespunzătoare de creare/anihilare din $\hat{\psi}(x)$, $\hat{\bar{\psi}}(x)$ și $\hat{A}_\mu(x)$

$$\hat{S}_{PP}^{(2)} = -e^2 \int d^4x_1 d^4x_2 N \left[\begin{array}{cccccc} \text{crea.} & \text{anih.} & & & \text{anih.} & \text{crea.} \\ e^- & \gamma & & & \gamma & e^+ \\ \downarrow & \downarrow & & & \downarrow & \downarrow \\ \left(\hat{\bar{\psi}}_{x_1}^+ \right) & \left(\hat{A}_{x_1}^- \right) & \underbrace{\left(\hat{\psi}_{x_1}^- \right) \left(\hat{\bar{\psi}}_{x_2}^+ \right)}_{iS_F(x_1-x_2)} & & \left(\hat{A}_{x_2}^- \right) & \left(\hat{\psi}_{x_2}^+ \right) \end{array} \right]$$

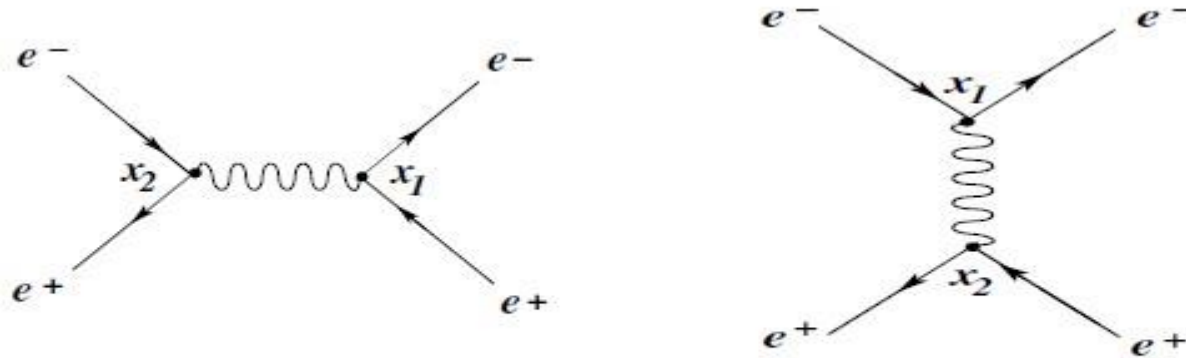
5.8 Evaluation Feynman Diagrams Moller Scattering: $e^- e^- \rightarrow e^- e^-$



- Folosind componentele corespunzătoare de creare/anihilare din $\hat{\psi}(x)$, $\hat{\bar{\psi}}(x)$ și $\hat{A}_\mu(x)$

$$\hat{S}_{mse}^{(2)} = -e^2 \int d^4x_1 d^4x_2 N \left[\begin{array}{cccc} \text{crea.} & \text{anih.} & & \text{crea.} & \text{anih.} \\ e^- & e^- & & e^- & e^- \\ \downarrow & \downarrow & & \downarrow & \downarrow \\ \left(\hat{\bar{\psi}}_{x_1}^+ \right) & \left(\hat{\psi}_{x_1}^- \right) & \underbrace{\left(\hat{A}_{x_1}^- \right) \left(\hat{A}_{x_2}^+ \right)}_{iD_F(x_1-x_2)} & \left(\hat{\bar{\psi}}_{x_2}^+ \right) & \left(\hat{\psi}_{x_2}^- \right) \end{array} \right]$$

5.9 Evaluation Feynman Diagrams Bhabha Scattering: $e^- e^+ \rightarrow e^- e^+$



$$\langle e^-, e^+ | \hat{S}_A | e^-, e^+ \rangle + \langle e^-, e^+ | \hat{S}_B | e^-, e^+ \rangle$$

- Folosind componentele corespunzătoare de creare/anihilare din $\hat{\psi}(x)$, $\hat{\bar{\psi}}(x)$ și $\hat{A}_\mu(x)$

$$\hat{S}_A = -e^2 \int d^4x_1 d^4x_2 N \left[\begin{array}{cccccc} \text{crea.} & \text{crea.} & & & \text{anih.} & \text{anih.} \\ e^- & e^+ & & & e^+ & e^- \\ \downarrow & \downarrow & & & \downarrow & \downarrow \\ \left(\hat{\bar{\psi}}_{x_1}^+ \right) & \left(\hat{\psi}_{x_1}^+ \right) & \underbrace{\left(\hat{A}_{x_1}^- \right) \left(\hat{A}_{x_2}^+ \right)}_{iD_F(x_1-x_2)} & & \left(\hat{\bar{\psi}}_{x_2}^- \right) & \left(\hat{\psi}_{x_2}^- \right) \end{array} \right]$$

$$\hat{S}_B = -e^2 \int d^4x_1 d^4x_2 N \left[\begin{array}{cccccc} & \text{anih.} & \text{crea.} & & \text{crea.} & \text{anih.} \\ & e^- & e^- & & e^+ & e^+ \\ & \downarrow & \downarrow & & \downarrow & \downarrow \\ & \left(\hat{\bar{\psi}}_{x_1}^- \right) & \left(\hat{\psi}_{x_1}^+ \right) & \underbrace{\left(\hat{A}_{x_1}^- \right) \left(\hat{A}_{x_2}^+ \right)}_{iD_F(x_1-x_2)} & \left(\hat{\psi}_{x_2}^+ \right) & \left(\hat{\bar{\psi}}_{x_2}^- \right) \end{array} \right]$$

5.10 Feynman Diagrams Evaluation for Nonlinear SF-QED Processes

Linear, single-photon QED interaction processes described by Feynman diagrams presented before, can be studied in the multi-photon regime using the same Feynman diagrams, but with "dressed" (Dirac-Volkov) particle states and propagators, because the particle is moving in the oscillating EM field.

The **Strong Field Feynman rules** are summarized in [54]:

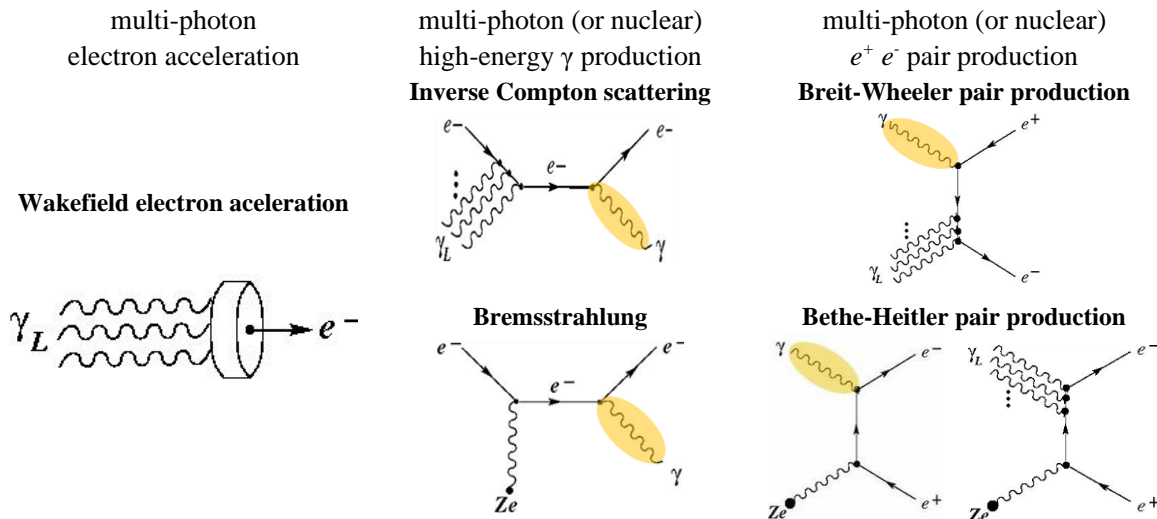
1. External incoming or outgoing electrons with momentum p are represented by laser **dressed Dirac-Volkov state** $\hat{\psi}(x)$ or $\hat{\bar{\psi}}(x)$ respectively.
2. For incoming and outgoing positrons, one uses the corresponding negative energy **dressed Dirac-Volkov states**.
3. An internal fermion line corresponds to the **Dirac-Volkov propagator**.
4. Internal and external photon lines are translated into the **free photon propagator** and the **free photon states**, respectively.
5. Each interaction vertex corresponds to a factor $-ie\gamma_\mu$ and an integral d^4x .
6. Symmetry factors for identical particles are the same as in usual QED.

5.11 SF-QED with dressed electron

The motion of a free electron in an EM field can be described in terms of the interaction of the electron with a classical plane wave of frequency ω . In general, such an electron has an oscillatory motion with the same frequency ω and will radiate in turn. It behaves as if it had an effective mass: $\bar{m}_e = m_e \sqrt{1 + \xi^2}$ and appears in the quantum treatment of the solutions of the Dirac equation for free electrons in the EM plane wave as the field Dirac – Volkov “dressed” states and propagators, with electron effective mass \bar{m}_e and effective 4-momentum

$$q_\mu = p_\mu + \frac{\xi^2 m^2}{2(k \cdot p)} k_\mu \quad \text{where } k_\mu \text{ is the wave (laser) photon 4-momentum.}$$

To study the SF-QED processes it is necessary to draw the corresponding Feynman diagrams with dressed particles. Then, evaluation of the Feynman diagrams allows to determine the invariant amplitude and the S matrix elements, using the electromagnetic $A_\mu(x)$ and Dirac $\hat{\psi}(x)$ and $\hat{\bar{\psi}}(x)$ field operators with the corresponding Fourier annihilation and creation components. Finally, the cross section could be calculated for experimental design.



Outline

1. Introduction
2. Vacuum interactions – Schwinger effect
3. QED interaction processes (theory & exp.)
4. ELI-NP Experiments for SF-QED study
5. Physics of the QED processes at ELI-NP
6. Task Force, plan and resources

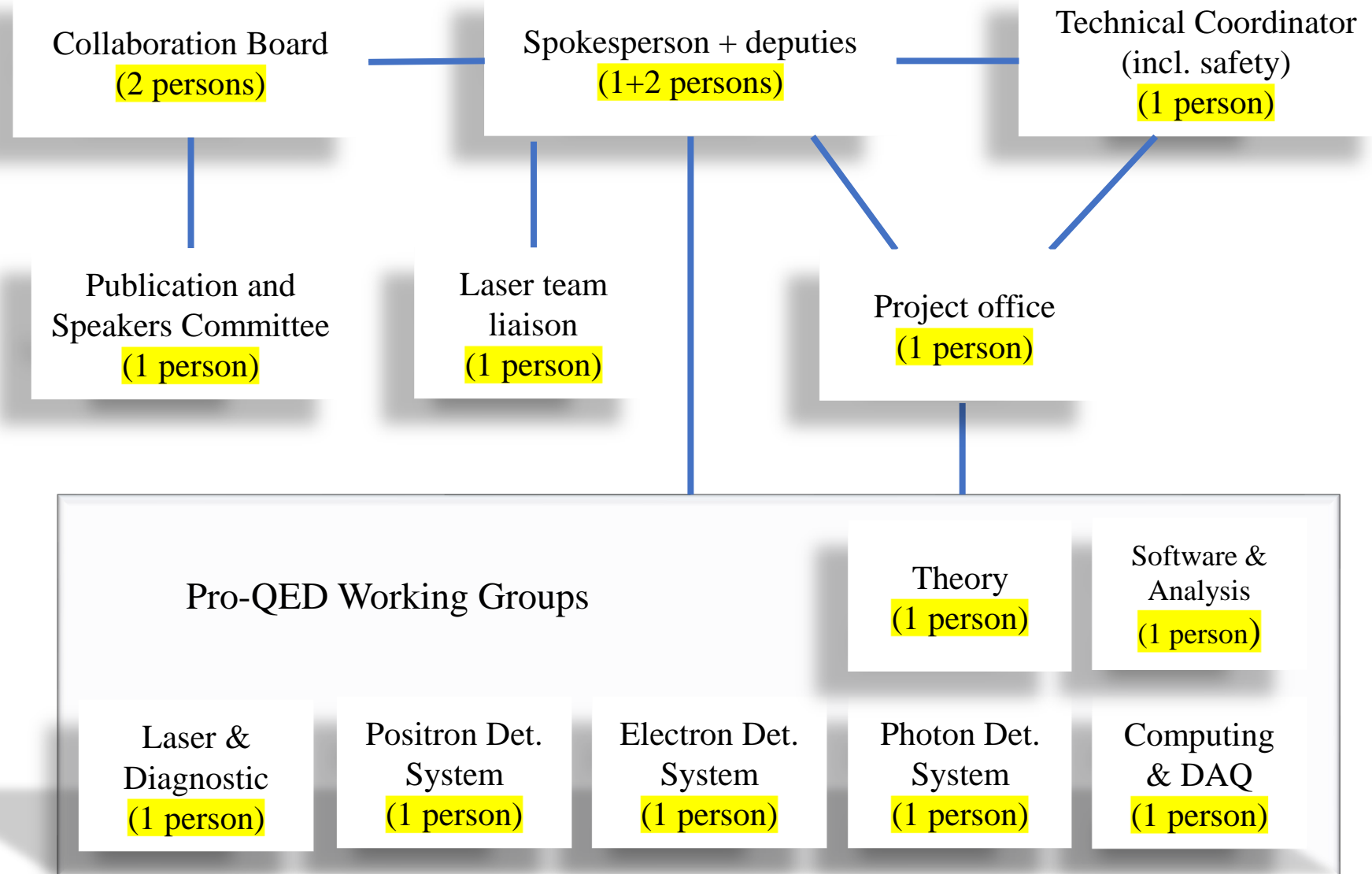
7.1 SF-QED Task Force plan

The experimental project assumes an international Task Force team to organize workshops, conferences and finally to prepare Letter of Intent, Conceptual Design Report and Technical Design Report.

Theoretical, Simulation & Experimental tasks:

- **Cross section** for SF-QED processes by **Feynman diagrams with Volkov states**
- **Events generator of the physical process** on the final states **phase space**
- **Characteristic theoretical distributions** of the physical process
- **Detector simulation response** and plot characteristic parameter distributions
- **Experimental setup** description and the setup detection parameters
- **Particle transport** and detector signal simulation
- **Data acquisition** and measuring process
- **Data analysis and plot** of measured physical quantities
- **Real and background events selection** with trigger and cut conditions on the ntuple experimental spectra
- **Evaluation, interpretation and publication of the results**

Organizational Chart



Conclusion

(text presented for the Booklet, not yet published <https://www.ifa-mg.ro/eli/brosura.php>)

We would like to involve our institution and bring forth the topic of nonperturbative QED at ELI-NP.

The Pro-QED project proposed vacuum Strong Field QED (SF-QED) interaction processes to be studied at the ELI-NP laser light infrastructure <https://arxiv.org/pdf/2307.09315.pdf>.

The investment for ELI-NP took into account the study of SF-QED, presented long time ago in the *ELI-NP White-Book* <https://www.eli-np.ro/whitebook.php>, page 7, under "Basic Science" and underlined as first priority for: "Fundamental physics of perturbative and non-perturbative high-field QED: pair creation, high energy γ rays ...".

The studies of fundamental interactions in Electrodynamics always were of high interest and awarded with Nobel Prizes (see **Slide 4**). In 2023, the Nobel Prize in physics was awarded to a specific subject explored at ELI-ALPS (Hungary) laser pillar. The topic was presented in the *ELI-ALPS White-Book*

https://www.eli-alps.hu/files/Documents/file_eng/ELI-Book_low_res_version_1.pdf.

Now, the ELI-NP, with such equipment, could realistically be the next nominee. The record laser power of 10 PW was achieved and now is ready for transition to the SF-QED experiments, able to capitalize on this unique asset. Meanwhile, **the topic has become of great interest worldwide**, see <https://journals.aps.org/rmp/pdf/10.1103/RevModPhys.94.045001>.

With the development of high-power lasers, similar works began to be prepared in other research centers, see **Slide 17** <https://arxiv.org/abs/1905.00059v1> and ELI-NP is seen as an important competitor.

Now there is a race against the clock and Romania could win, as it has the most powerful laser in the world.

The SF-QED interaction processes study is conditioned by the record power of 10 PW of the ELI-NP as to reach a sufficiently strong field, close to Schwinger critical threshold $E_{cr} = 1.3 \cdot 10^{18}$ V/m.

The possibility to turn light into matter, suggested almost 90 years ago by G. Breit & J. A. Wheeler, *Collision of two light quanta*, Phys. Rev. 46(12), 1087 (1934), can now be tested experimentally, benefiting from the laser light intensity available at ELI-NP.

Conclusion

The ELI-NP laser's top performances to be used in SF-QED experiments, include (see **Slide 13**)

- Laser Wakefield Acceleration (LWFA) of the electrons at high energy, GeV order.
- Production of high-energy gamma photons, of GeV order (inverse Compton and Bremsstrahlung)
- Light-matter conversion (Breit-Wheeler or Bethe-Heitler processes) as e^+e^- pair creation from light.

We hope our proposal will find the interest and support of the public research institutions in Romania.

The experimental works, on vacuum Strong Field QED interaction processes, at ELI-NP, include:

- **Systematic studies** of the dynamics of fundamental SF-QED processes possible to approach at ELI-NP
- **Evaluation of the amplitude and cross section**, using Feynman diagrams with electron and photon quantum fields and propagators in strong EM field, for the processes: γ -e inverse Compton scattering, Breit-Wheeler e^+e^- pair production, Bethe-Heitler e^+e^- pair production, Dirac e^+e^- pair annihilation, e^-e^- Moller Scattering, e^+e^- Bhabha Scattering, Electron Self Energy, Photon Self Energy, Vacuum Energy.
- **Designing experimental works** to measure some fundamental SF-QED processes, using high-power lasers at ELI-NP
- **Carrying out experimental works** to measure physical properties related to the production of e^+e^- pairs (Schwinger mechanism) in the photon-multiphoton interaction (nonlinear Breit-Wheeler), the multiphoton-virtual photon interaction of the nucleus field (nonlinear Bethe-Heitler).

The project proposes an Organizational Chart for the scientific staff of the experimental works.

We hope our proposal will find the interest and support of the public research institutions in Romania.

Thank you

References

- [1] F. Sauter, “Über das Verhalten eines Elektrons im homogenen elektrischen Feld nach der relativistischen Theorie Diracs“ Z. Phys. 69 (1931) 742;
W. Heisenberg, H. Euler, „Folgerungen aus der Diracschen Theorie des Positrons“ Z. Phys. 98 (1936) 714;
J. S. Schwinger, „On Gauge Invariance and Vacuum Polarization“, Phys. Rev. 82, 664 (1951).
- [2] G. Breit and J.A. Wheeler, “Collision of Two Light Quanta”, Phys. Rev. 46, 1087 (1934).
- [3] H.A. Bethe and W. Heitler, “On the stopping of fast particles and on the creation of positive electrons”, Proc. Roy. Soc. A146, 83 (1934).
- [3] H. R. Reiss, “Absorption of light by light”, J. Math. Phys. 3, 59 (1962).
- [4] N. B. Narozhny, A. I. Nikishov, and V. I. Ritus, “Quantum Processes in the Field of a Circularly Polarized Electromagnetic Wave”, Sov. Phys. JETP 20, 622 (1965).
- [5] V. I. Ritus, “Quantum effects of the interaction of elementary particles with an intense electromagnetic field”, J. Sov. Laser Res. 6, 497 (1985).
- [7] O.C. De Jager et al., “Estimate of the intergalactic infrared radiation field from γ -ray observations of the galaxy Mrk421”, Nature 369, 294 (1994).
- [8] O. Pike – interview “Light into matter”, Nature Photonics, Vol 8, 2014
- [9] D. B. Blaschke et al., “Influence of Laser Pulse Parameters on the Properties of e^-e^+ Plasmas Created from Vacuum”, Contrib. Plasma Phys. 53, 165 (2013).
- [10] A. I. Titov, B. Kampfer, H. Takabe, and A. Hosaka, “Breit-Wheeler process in very short electromagnetic pulses”, Phys. Rev. A 87, 042106 (2013)
- [11] G. V. Dunne, H. Gies, and R. Schutzhold, “Catalysis of Schwinger vacuum pair production”, Phys. Rev. D 80, 111301 (2009).
- [12] P. H. Bucksbaum, G. V. Dunne et al., „Understanding the Fully Non-Perturbative Strong-Field Regime of QED” SNOWMASS-2021, LoI to Theory Frontier (2020).
- [13] C. Bula et al. [E144], “Observation of nonlinear effects in Compton scattering,” Phys. Rev. Lett. 76, 3116-3119(1996)
- [14] D. Burke et al. [E144], “Positron production in multi-photon light by light scattering”, Phys. Rev. Lett. 79, 1626-1629 (1997)
- [15] M. Altarelli, R. Assmann, F. Burkart, B. Heinemann, T. Heinzl, T. Koffas, A. Maier, D. Reis, A. Ringwald and M. Wing, “Summary of strong-field QED Workshop”, arXiv:1905.00059 (2019).
- [16] H. Abramowicz et al., “Letter of Intent for the LUXE Experiment”, arXiv:1909.00860 (2019).
- [17] S. Meuren on behalf of the E-320 Collaboration, “Probing Strong-field QED at FACET-II (SLAC E-320)” (2019)
- [18] I. Turcu et al, “High field physics and QED experiments at ELI-NP”, Rom. Rep. Phys. 68, Supplement, S145 (2016).

References

- [19] R. Falcone, F. Albert, F. Beg, S. Glenzer, T. Ditmire, T. Spinka, and J. Zuegel, “*Workshop Report: Brightest Light Initiative*”, arXiv:2002.09712 (2020).
- [20] S. Baalrud, N. Ferraro, L. Garrison, N. Howard, C. Kuranz, J. Sarff, E. Scime, and W. Solomon, “*A Community Plan for Fusion Energy and Discovery Plasma Sciences – Report of the 2019–2020 American Physical Society Division of Plasma Physics Community Planning Process*”, APS-DPP-CPP, 1-186 (2020).
- [21] S. Meuren, P. H. Bucksbaum, N. J. Fisch, F. Fiúza, S. Glenzer, M. J. Hogan, K. Qu, D. A. Reis, G. White and V. Yakimenko, “*On Seminal HEDP Research Opportunities Enabled by Colocating Multi-Petawatt Laser with High-Density Electron Beams*”, arXiv:2002.10051 (2020).
- [22] V. Yakimenko, S. Meuren, F. Del Gaudio et al., “*Prospect of Studying Nonperturbative QED with Beam-Beam Collisions*”, Phys. Rev. Lett. 122, no.19, 190404 (2019).
- [23] 2019 SLAC workshop: Physics Opportunities at a Lepton Collider in the Fully Nonperturbative QED Regime.
- [23] Extremely High Intensity Laser Physics Conference: EXHILP 2019.
- [24] Greiner W. and Reinhardt J. 2008 „Quantum Electrodynamics“ (Berlin: Springer)
- [25] B Kettle et al. ”*A laser–plasma platform for photon–photon physics: the two photon Breit–Wheeler process*” *New J. Phys.* **23** 115006, (2021)
- [26] Bula C. et al, “*Observation of Nonlinear Effects in Compton Scattering*” (SLAC), Phys.Rev.Lett. 76 3116 (1996)]
- [27] Bula C. (E-144 SLAC), “*Positron Production in Multiphoton Light-by-Light Scattering*” AIP Conference Proceedings 396, 165 (1997)
- [28] Hui Chen et al., “*Relativistic Positron Creation Using Ultraintense Short Pulse Lasers*”, Phys. Rev. Lett. 102, 105001 (2009).
- [29] M. Jirka et al., “*Electron dynamics and γ and e^-e^+ production by colliding laser pulses*”, Phys. Rev. E 93, 023207 (2016).
- [30] J. M. Cole, et al., “*Experimental evidence of radiation reaction in the collision of a high-intensity laser pulse with a laser-wakefield accelerated electron beam*”, Phys. Rev. X 8, 011020 (2018).
- [31] Hartin, A. Ringwald, and N. Tapia, “*Measuring the boiling point of the vacuum of quantum electrodynamics*”, Phys. Rev D 99, 036008 (2019)
- [32] T. N. Wistisen, A. Di Piazza, H. V. Knudsen, and U. I. Uggerhøj, “*Experimental evidence of quantum radiation reaction in aligned crystals*”, Nat. Commun. 9, 795 (2018)
- [33] K. Poder et al., “*Experimental signatures of the quantum nature of radiation reaction in the field of an ultraintense laser*”, Phys. Rev. X 8, 031004 (2018).
- [34] W. Heitler, “*The Quantum Theory of Radiation*” (Clarendon Press, Oxford, 1954)]

References

- [35] E. P. Liang, S. C. Wilks, M. Tabak, “*Pair Production by Ultraintense Lasers*”, Phys. Rev. Lett. 81, 4887 (1998).
- [36] B. Shen and J. Meyer-ter-Vehn, “*Pair and γ -photon production from a thin foil confined by two laser pulses*”, Phys. Rev. E 65, 016405 (2001).”,
- [37] P. L. Shkolnikov et al., “*Positron and gamma-photon production and nuclear reactions in cascade processes initiated by a sub-terawatt femtosecond laser*”, Appl. Phys. Lett. 71, 3471 (1997).
- [38] D. A. Gryaznykh, Y. Z. Kandiev, and V. A. Lykov, “*Estimates of electron-positron pair production in the interaction of high-power laser radiation with high-Z targets*”, JETP Lett. 67, 257 (1998).”,
- [39] V. I. Berezhiani, D. P. Garuchava, and P. K. Shukla, “*Production of electron–positron pairs by intense laser pulses in an overdense plasma*”, Phys. Lett. A 360, 624 (2007).
- [40] T. E. Cowan et al., “*High energy electrons, nuclear phenomena and heating in petawatt laser-solid experiments*” Laser and Particle Beams 17, 773 (1999).
- [41] C. Gahn et al., “*Generating positrons with femtosecond-laser pulses*”, Appl. Phys. Lett. 77, 2662 (2000)
- [42] I. C. E. Turcu et al., “*Quantum electrodynamics experiments with colliding petawatt laser pulses*”, High Power Laser Science and Engineering, (2019), Vol. 7, <https://doi.org/10.1017/hpl.2018.66>
- [43] F. Negoita, et al. “*Laser Driven Nuclear physics at ELI-NP*”, Rom. Rep. Phys. 68, S37 (2016).
- [44] S. Gales, et al., “*The extreme light infrastructure-nuclear physics (ELI-NP) facility: new horizons in physics with 10 PW ultra-intense lasers and 20 MeV brilliant gamma beams*”, Rep. Prog. Phys. 81, 094301 (2018)
- [45] J. Wardle et al., “*Electron–positron jets associated with the quasar 3C279*”, Nature (London) 395, 457 (1998).
- [46] P. Meszaros, “*Theories of Gamma-Ray Bursts*”, Annual Rev. Astron. Astrophys. 40, 137 (2002).
- [47] H. A. Weldon, “*Measuring T_c of the quark-gluon plasma with e^+e^- pairs*”. Phys. Rev. Lett. 66, 293 (1991).
- [48] E. G. Blackman and G. B. Field, “*Ohm’s law for a relativistic pair plasma*”, Phys. Rev. Lett. 71, 3481 (1993).
- [49] A. Gonoskov, T. G. Blackburn, and M. Marklund, “*Charged particle motion and radiation in strong electromagnetic fields*”, Rev. Mod. Phys., 94. 045001 (Oct–Dec 2022).
- [50] Kun Xue et al, “*Generation of arbitrarily polarized GeV lepton beams via nonlinear Breit-Wheeler process*”, Fundamental Research 2 (2022) 539-545
- [51] Y. I. Salamin, S.X. Hu, K.Z. Hatsagortsyana, C.H. Keitel, “*Relativistic high-power laser–matter interactions*”, Phys. Rep. 427 (2006) 41
- [52] D.L. Burke et al., “*Positron Production in Multiphoton Light-by-Light Scattering*” Phys. Rev. Lett. 79 (1997) 1626.
- [53] C. Bamber et al., “*Studies of nonlinear QED in collisions of 46.6 GeV electrons with intense laser pulses*”, Phys. Rev. D 60 (1999) 092004.
- [54] D. Seipt, “*Volkov States and Non-linear Compton Scattering in Short and Intense Laser Pulses*”, <https://arxiv.org/pdf/1701.03692.pdf> (2017)

Electromagnetic spectrum

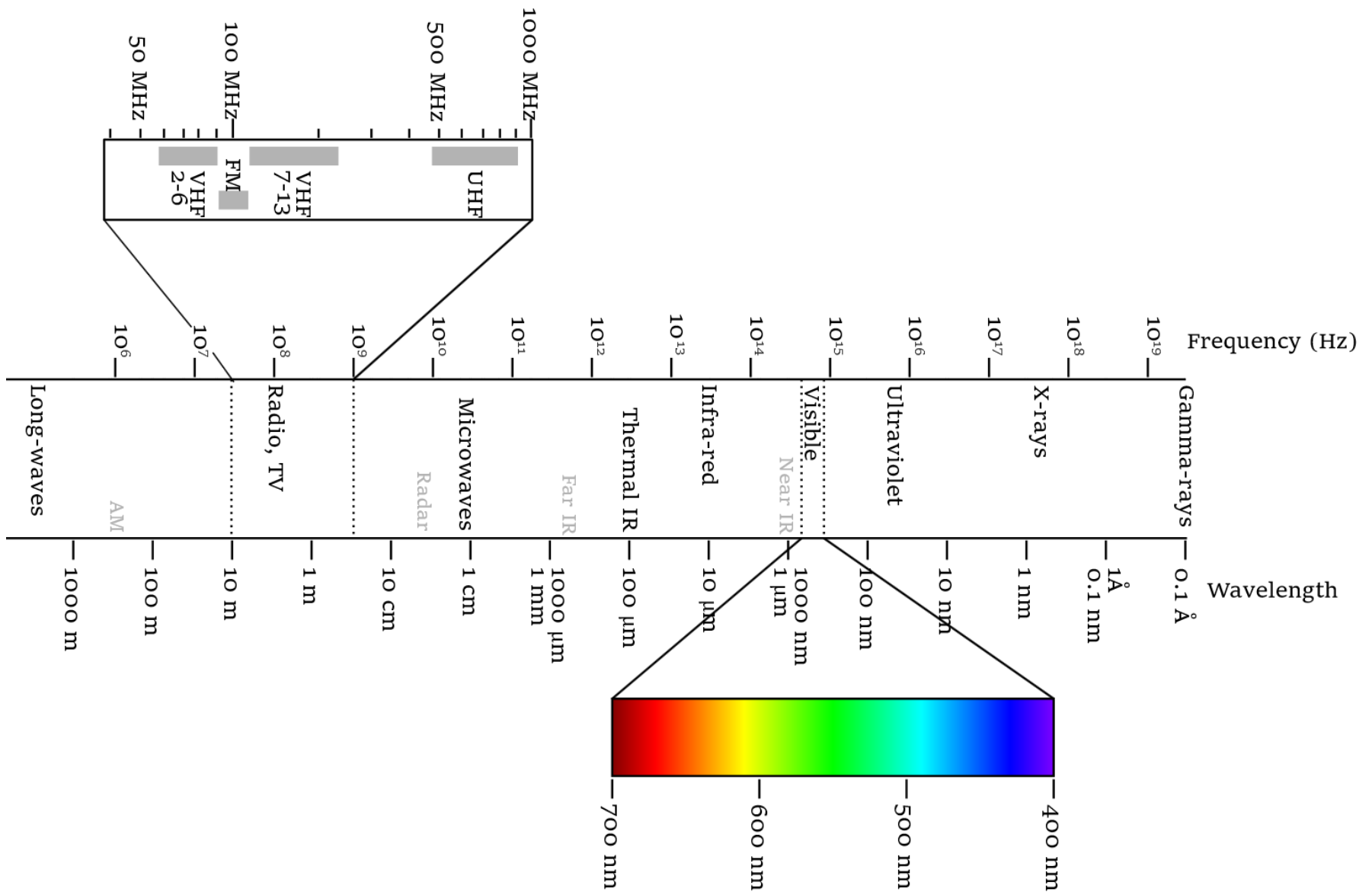


TABLE II. Parameters of the laser facilities shown in Fig. 2.

Name	Facility	Country	Wavelength (μm)	Energy (J)	Duration (fs)	Power (PW)
Station of Extreme Light	SIOM	China	0.9	1500	15	100
EP-OPAL	LLE	USA	0.8	500	20	25
SULF	SIOM	China	0.8	220	21	10
Apollon (F1)	LULI	France	0.82	150	15	10
PEARL-X	IAP	Russia	0.527	200	20	10
L4	ELI-Beamlines	Czechia	1.057	1500	150	10
HPLS	ELI-NP	Romania	0.814	200	20	10
J-EPOCH	ILE + QST	Japan	0.8	200	20	10
SULF (current)	SIOM	China	0.8	130	24	5.4
SG-II 5 PW	SIOM	China	0.808	150	30	5
CAEP-PW	CAEP	China	0.8	91	19	4.8
CoReLS	IBS	South Korea	0.8	83	20	4.15
ZEUS	CUOS	USA	0.8	60	20	3
ATLAS-3000	CALA	Germany	0.8	60	25	2.4
Qiangguang	SIOM	China	0.8	52	26	2
SG-II 5 PW	SIOM	China	0.808	37	21	1.8
Apollon	LULI	France	0.82	38	22	1.7
Nova Petawatt	LLNL	USA	1.054	660	440	1.5
BELLA	LBNL	USA	0.8	40	30	1.3
LFEX	GEKKO XII	Japan	1.054	2000	1500	1.3
J-KAREN-P	KPSI	Japan	0.82	40	30	1.3
PETAL	CEA	France	1.053	850	700	1.2
Xtreme Light III	NLCM	China	0.8	32	28	1.1
CoReLS	IBS	South Korea	0.8	33	30	1.1
Z-Petawatt	Sandia	USA	1.054	500	500	1
Vulcan Petawatt	CLF, RAL	UK	1.054	500	500	1
Orion	AWE	UK	1.053	500	500	1
Apollon (F2)	LULI	France	0.82	15	15	1
PEneLOPE	HZDR	Germany	1.03	150	150	1
VEGA-3	CLPU	Spain	0.8	30	30	1
CETAL	INFLPR	Romania	0.8	25	25	1
L2	ELI-Beamlines	Czechia	0.82	15	15	1
L3 (HAPLS)	ELI-Beamlines	Czechia	0.82	30	30	1
SG-II UP (Shenguang II)	SIOM	China	1.054	1000	1000	1
PWM (Petawatt Module)	GEKKO XII	Japan	1.054	420	470	0.89
Texas Petawatt	Univ. of Texas at Austin	USA	1.057	120	140	0.86
J-KAREN	KPSI	Japan	0.8	28	33	0.85
Xingguang-III (fs beam)	LFRC	China	0.8	20	27	0.74
OMEGA-EP (short pulse)	LLE	USA	1.053	500	700	0.71
Diocles	ELL	USA	0.8	20	30	0.67
NIF	LLNL	USA	0.3516	1.80×10^6	3.00×10^6	0.6
PEARL	IAP	Russia	0.91	24	45	0.53

TABLE II. (Continued)

Name	Facility	Country	Wavelength (μm)	Energy (J)	Duration (fs)	Power (PW)
HERCULES	CUOS	USA	0.8	15	30	0.5
Gemini	CLF	UK	0.8	15	30	0.5
Laser Megajoule	CEA	France	0.351	1.50×10^6	3.00×10^6	0.5
PHELIX	HI GSI	Germany	1.054	200	400	0.5
Titan (west)	LLNL	USA	1.053	300	700	0.43
SCAPA	Univ. of Strathclyde	UK	0.8	8.75	25	0.35
Scarlet	Ohio State Univ.	USA	0.8	10	30	0.33
Jeti200	HI Jena	Germany	0.8	4	17	0.24
ALEPH	Colorado State Univ.	USA	0.4	10	45	0.2
POLARIS	HI Jena	Germany	1.03	17	98	0.17
Arcturus	Heinrich-Heine Univ.	Germany	0.8	3.5	30	0.12
DRACO	HZDR	Germany	0.8	3.5	30	0.12

Today experiments on radiation emission and pair creation in the strong-field regime form part of the planned experimental programs at almost every major petawatt or multi petawatt laser facility, including the

- Extreme Light Infrastructure (ELI) (Weber et al., 2017; Gales et al., 2018),
- Apollon (Papadopoulos et al., 2016),
- Station of Extreme Light (Cartlidge, 2018),
- Center for Relativistic Laser Science (CoReLS) (Yoon et al., 2021),
- J-KAREN-P (Kiryama et al., 2020),
- Omega Laser Facility (Bromage et al., 2019),
- Zetawatt-Equivalent Ultrashort Pulse Laser System (ZEUS) (Nees et al., 2020),
- conventional accelerator facilities (Abramowicz et al., 2019; Meuren, 2019).

(A. Gonoskov, T. G. Blackburn, and M. Marklund, S. S. Bulanov, **REVIEWS OF MODERN PHYSICS, VOLUME 94, OCTOBER–DECEMBER 2022.**)